CAPACITY OF GROUT-FILLED STEEL BEAM UNDER FLEXURAL CYCLIC LOAD

NGAN YEW TENG

CIVIL ENGINEERING
UNIVERSITI TEKNOLOGI PETRONAS
JUNE 2010

Capacity of Grout- Filled Steel Beam under Flexural Cyclic Load

by

Ngan Yew Teng

Dissertation submitted in partial fulfilment of
the requirements for the
Bachelor of Engineering (Hons)
(Civil Engineering)

JUNE 2010

Universiti Teknologi PETRONAS
Bandar Seri Iskandar
31750 Tronoh
Perak Darul Ridzuan

CERTIFICATION OF APPROVAL

Capacity of Grout- Filled Steel Beam under Flexural Cyclic Load

by

Ngan Yew Teng

A project dissertation submitted to the
Civil Engineering Programme
Universiti Teknologi PETRONAS
in partial fulfilment of the requirement for the
BACHELOR OF ENGINEERING (Hons)
(CIVIL ENGINEERING)

Approved by,

(AP. Dr. Narayanan Sambu Potty)

UNIVERSITI TEKNOLOGI PETRONAS
TRONOH, PERAK
January 2010

CERTIFICATION OF ORIGINALITY

This is to certify that I am responsible for the work submitted in this project, that the original work is my own except as specified in the references and acknowledgements, and that the original work contained herein have not been undertaken or done by unspecified sources or persons.

NGAN YEW TENG

ABSTRACT

In civil engineering applications, hollow section beams are extensively used mainly in the construction industry and offshore structures. After several years of usage, the structures undergo damage and suffer corrosion thus requiring regular maintenance. One of the methods to rectify this problem is infilling with grout in the steel hollow sections. This study is to determine the flexural behavior of grout-filled steel hollow section beams in offshore applications. The characteristics of the grout-filled steel beams which include high ductility, strength, and greater energy absorption capacity have made these composite beams become popular in civil engineering. Extensive research works to study the capacity of grout-filled steel beams have been carried out. However, studies on the behavior of grout-filled steel beams under flexural cyclic load have not been observed in the literature where such problem can arise when the moment induced during earthquakes and the vibration of the machineries could cause some effects on the beams which would reduce the service life of the beams. In the present study, therefore an attempt has been made to study the behavior of grout-filled steel beams subjected to flexural cyclic load under different parameters which include the D/t ratio and also the stiffness of the beams which would affect the bonding strength of the grout with the beams. The relationship between the different strength of flexural cyclic load and the number of cycles to failure would be investigated.

ACKNOWLEDGEMENT

In the first place I would like to record my gratitude to my supervisor, Associate Professor Dr. Narayanan Sambu Potty for his supervision, advice, and guidance from the very early stage of this research as well as giving me extraordinary experiences throughout the work. Above all and the most needed, he provided me unflinching encouragement and support in various ways. His truly engineer intuition has made him as a constant oasis of ideas and passions in science, which exceptionally inspire and enrich my growth as a student, a researcher and an engineer want to be. One simply could not wish for a better or friendlier supervisor.

In the various laboratories I have been aided for the one year in running the equipment by two fine lab technologists, Mr. Johan and Mr. Hafiz. The smooth running of the dynamic machine is much more a testament to their efforts than my own. Safety briefing from the beginning of the lab experiment, procedures in handling tools and materials during the lab experiment are well explained and monitored by these two experienced lab technologists. I express my gratitude to both of them and without their cooperation and patience this thesis, too, would not have been completed by time.

The Department of Civil Engineering has provided the support and equipment I have needed to produce and complete my thesis and the university has funded my studies.

Last but not least, I would like to thank my parents for supporting me throughout all my studies and their precious moral support during my undergraduate studies in the University.

TABLE OF CONTENTS

LIST OF TABLES

LIST OF FIGURES

CHAPTER 1

INTRODUCTION

1.1 Background of Study

In construction and offshore industries, hollow sections beams are widely used due to the characteristic of speed in construction. During their service life, the beams may suffer damage due to impact and corrosion and may need to be repaired.

The main cause of deterioration of infrastructures involving metallic structures is corrosion. Corrosion of steel beams in bridges becomes an alarming concern due to the maintenance of these structures is often being neglected. However in most cases, only certain part of the structures is affected and therefore only regular maintenance is required. Replacement alternative such as repair, upgrading and rehabilitation were employed as it requires less time and reduce service interruptions. However, a retrofit option remains the most economical alternative before considering in replacing the whole structure (Photiou, Hollaway, & Chryssanthopoulos, 2006).

A common retrofit option used is by strengthening the affected structures by using bolted steel cover plates but it is time consuming and often involved high labor cost (Phares, Wipf, Klaiber, Abu-Hawash, & Lee, 2003). Therefore, advanced composite materials have been introduced to the civil engineering application as it has been proven to reduce the environmental degradation. Among the development area of the composites is the repairing and upgrading of beams in bridges and buildings especially in the severe environment (Deng & Lee, 2007).

Concrete/grout -filled steel beam is categorized as composite beam where it has greater moment capacity compared with the reinforced concrete beams and the steel beams. The term "composite beam" refers to the steel tube and the infilled concrete/grout act compositely.

By filling the tubular steel beams with concrete/grout, it may be useful in withstanding larger moment as both infilled concrete/grout and the thin-walled tubular sections counter the weaknesses of one another.

Composite beams have been used in structures such as high rise buildings and offshore jacket members. One of the advantages of composite beam is it has greater energy absorbing capacity compared with the reinforced concrete beam and steel beam. Therefore, composite beams have been used in earthquake-resisting structures as they are able to absorb greater earthquake forces and thus reduce the damages to the whole structures.

1.2 Problem Statement

Steel tubular beams have widely been used in structural applications particularly in offshore and inland structures due to the steel characteristics such as high ductility, low mass-length ratio, and speed in construction. However, steels which are subject to continuously varying or alternating loads can fracture at values of stress considerably less than the ultimate value found during static test. This continuously varying or alternating load is known as cyclic load.

Experimental evidence has indicated that fluctuating stresses, in some cases smaller than the elastic limit, will induce fracture if repeated a sufficient number of times. This type of failure is called fatigue failure and is dependent on the number of cycles and the range of stress to which an element is subjected (McKenzie, 2004).

Some of the steel members which supporting heavy vibrating machinery and certain classes of crane supporting structures are subjected to fatigue failure. Therefore, these members should be checked for fatigue resistance.

Although the grout-filled steel beam is a better solution in resisting flexural load compared to the ordinary reinforced concrete beam and the steel beam, the capacity of the grout-filled steel tube and its behavior when subjected to flexural cyclic load has not been reported in literature.

The grout-filled steel beam might be a better alternative to increase the overall capacity of the beam under the influence of flexural load. However, the capability of grout-filled steel beam to withstand the cyclic load might be affected as the bonding strength of the grout with the beam might be decreased, resulting in debonding. This could result in reduction of flexural strength of the beam.

Therefore, further studies are needed to investigate the relationship between the overall capacity of the grout-filled steel beam and its behavior under the influence of flexural cyclic load and the number of cycles of the flexural cyclic load to cause failure.

1.3 Objectives

i) To compare the static lateral load capacity of bare and infilled tubular beams.

ii) To obtain the failure modes, overall capacity and behavior of grout-filled steel beam subjected to flexural cyclic load.

iii) To determine the influences of parameters such as D/t and span of the beam on the overall capacity of the grout-filled steel beams under flexural cyclic load.

iv) To determine the relationship between the stress range of the flexural cyclic load and the number of the cycles to failure.

1.4 Scope of Study

The scope of the research works is limited by the following in order to achieve the objectives within the time frame and also the budget allocated.

i) The sectional type for the beams to be used in this project would be circular hollow section (CHS) instead of rectangular hollow section (RHS). Circular hollow sections of 1) diameter= 6cm and 2) thickness = 3.2mm, 5.0mm have been used.

ii) For infilling beams, grout of strength 75 MPa has been used. A proprietary grout supplied by SIKA has been used.

iii) The spans of beams chosen for the tests are 1.2 m and 0.6 m.

CHAPTER 2

LITERATURE REVIEW

2.1 Methods of Strengthening Damaged Beams

In terms of increasing the carrying capacity and rehabilitation due to corrosion degradation, strengthening is performed to the required steel structures (Schnerch, Stanford, Sumner, & Rizkalla, 2005). During the previous years, the usage of steel plates and cables to strengthen the beams cause many drawbacks which includes additional weight and corrosion of steel plates that could affect the bond strength (Lee & Hausmann, 2004). In addition, current techniques of strengthening steel structures using bolting or welding steel plates to the existing structure is often not desirable due to the poor fatigue performance of welded connections (Schnerch, Stanford, Sumner, & Rizkalla, 2005). Recently, new methods of strengthening the damaged beams have been continuously produced by researchers worldwide. Among the method of strengthening are by using concrete infill and applying fiber-reinforced polymer composites.

2.2 Strengthening of Structural Elements Using Concrete Infilled

Composites comprise of two materials which are the reinforcing phase in the form of fiber, sheets or particles and the matrix phase in which the reinforcing phase is embedded. The characteristics of reinforcing materials are high strength with low densities while the matrix is usually ductile. The combination of these characteristics will produce a material with desirable properties owing to its high strength and ductility.

Nowadays, hot-rolled steel or reinforced concrete is substituted with the steel-concrete composite in the construction of small-to medium sized buildings. The steel-concrete composite consists of beams comprising hollow steel elements with an infill of concrete (Soundararajan & Shanmugasundaram, 2008). The usage of composite is mostly developed in the construction industry due to the ease of fabrication and its high strength characteristic besides being more economical (Gho & Liu, 2003). This combination will force the steel and concrete to act together thus shifting the neutral axis of the section upwards. Therefore, the concrete will be in compression and the steel will endure the tension. This in turn will make the beam stiffer and lessen the deflection of the composite beams (Soundararajan & Shanmugasundaram, 2008).

The strength and ductility of the composite is enhanced by the steel hollow section as the steel constrained the volume increase in the core concrete caused by the cracks. High-strength steel hollow sections provide better strength and ductility performance while high-strength concrete contributes larger stiffness to the column (Gho & Liu, 2003).

Investigations were done to determine the flexural behaviour of twelve 1600-mm-long high-strength rectangular concrete-filled steel hollow section (CFSHS) specimens tested to failure under pure bending. The author concluded that all the specimens demonstrate post-yield behavior with good ductility performance.

Beams, filled with different types of concrete, were capable of developing the full flexural strength of their sections. Moreover, these types of concrete enhance the ultimate moment capacity of the steel hollow sections. It can also be concluded that the failure mechanism of the beam sections result in an excessive deflection with no lateral disturbances or any other form of instability (Soundararajan & Shanmugasundaram, 2008).

2.3 Analysis for Non-strengthened and Strengthened Beams

This section would be divided into two parts which is the non strengthened beams and beams strengthened using concrete. Further explanations are as follows:

2.3.1 Non Strengthened Beams:

BS5950 Part 1 provides the methodology for calculating the shear capacity and moment capacity of steel beam. They are explained below.

Shear capacity

The shear force F_v should not be greater than shear capacity P_v where $P_v = 0.6p_yA_v$ and A_v is the shear area taken as follows related to this study:

For circular hollow sections

$A_v = 0.6A$

Moment capacity, M_c with low shear load

Where $F_v \leq 0.6P_v$ the moment capacity, M_c, should be taken as follows.

(1) For plastic or compact sections:

$$M_c = p_yS \text{ but} \leq 1.2p_yZ$$

(2) For semi-compact sections:

$$M_c = p_yZ$$

(3) For slender sections:

$$M_c = p_yZ$$

Where

p_y is the design strength

S is the plastic modulus of the section about the relevant axis

Z is the elastic modulus of the section about the relevant axis

Moment capacity with high shear load

Where $F_v > 0.6P_v$ the moment capacity, M_c, should be taken as follows.

(1) For plastic or compact sections:

$$M_c = p_y(S\text{-}\rho S_v) \text{ but} \leq 1.2\, p_y Z$$

$$\text{Where } \rho = [2(F_v/P_v)\text{-}1]^2$$

and S_v is taken as follows:

For sections with equal flanges S_v is the plastic modulus of the shear area, A_v

For sections with unequal flanges; $S_v = S\text{-}S_f$ in which S_f is the plastic modulus of the effective section excluding the shear area A_v.

(2) For semi-compact sections:

$$M_c = p_y Z$$

(3) For slender sections:

$$M_c = p_y Z$$

2.3.2 Beams strengthened using concrete:

The ultimate moment capacity, M_u, is determined by summing the moments in the steel tube and concrete core, given as:

$$M_u = M_{cc} + M_{st} + M_{sc}$$

where; M_{cc} is the moment created by the concrete in compression

M_{st} is the moment created by the steel in tension

M_{sc} is the moment created by the steel in compression

Equilibrium dictates that:

$$M_{cc} = 2/3\ f_c r_i^3 \cos^3 \gamma_o$$

$$M_{st} = M_{sc} = 2 f_y r_m^2 t \cos \gamma_o$$

where γ_o is the angular location of the plastic neutral axis, which is given as:

$$\gamma_o = \frac{\frac{\pi}{4}\left(\frac{f_c r_i^2}{f_y r_m t}\right)}{2 + \frac{1}{2}\left(\frac{f_c r_i^2}{f_y r_m t}\right)}$$

where; f_c is the compressive strength of the concrete

r_i is the inner radius of the steel tube

f_y is the steel yield strength

r_m is the average radius of the steel tube

t is the wall thickness

2.4 Cracking Patterns and Strength of Concrete- Filled Tubes (CFTs) under Different Moment Gradients

Concrete- filled tubes (CFTs) provide an efficient system reinforced concrete beams and can lead to rapid construction. The tube is essentially a structural form for the concrete core. Flexural behavior of CFT beams with steel tubes has been extensively studied. The studies demonstrated the remarkable ductility of the system and showed that concrete core changes the buckling mode of the tube in the compression side. (Shawkat, Fahmy, & Fan, 2008)

In these studies, it was found that classic shear failure (i.e. by means of major diagonal cracking) may never occur in CFT beams, unless the concrete is internally reinforced in the longitudinal direction.

2.5 The Behavior of Steel- Concrete Composite Beams under Repeated Load

An early crack initiation and subsequent crack propagation occurs at the weld collar of headed shear studs transferring the longitudinal shear forces between steel and concrete when subjected to cyclic load. This result in a decrease of the static and fatigue resistance of composite steel- concrete structures should not be considered as separate limit states which is the case in most design codes (Hanswille, Porsch, & Ustundag, 2007).

Steel-concrete composite beams are today widely used for bridges and industrial buildings. The transfer of longitudinal shear forces at the interface between both components is most realized by headed shear studs. Especially in bridges these shear studs are subjected to a steadily rising number of high- cycle loads, which may result in fatigue failure during the lifetime of the structure.

The fatigue resistance is verified comparably to steel structures, based on the concept with nominal stress ranges and the linear damage accumulation rule according to Palmgen-Miner where effects of pre-damage due to high-cycle load are neglected.

From previous investigations (Oehlers, 1990) it is known, that cyclic load of headed shear studs leads to a decrease of static strength, so that the assumptions for independent limit states are not given. Because the design life of cyclic loaded headed shear studs is characterized by a significant change in deformation behavior and deterioration in strength the reliability index of steel-concrete composite structures subjected to fatigue load may fall below target values in codes.

2.6 Concrete-Filled Double Skin Steel Tubular (CFDST) Beam-Columns Subjected to Cyclic Load

In recent years, it was proposed by several researchers that concrete filled double skin steel tubes (CFDST) be studied for their strength as a column or a beam. Advantages of CFDST over fully concrete filled steel tubes (CFST) include: increase in section modulus; enhancement in stability; lighter weight; better damping characteristics and better cyclic performance. It is expected that the CFDST columns can obtain a higher fire resistance period than the CFST columns, due to the inner tubes of the composite columns being protected by the sandwiched concrete during fire. It is thus expected that concrete filled double skin steel tubes (CFDST) have the potential of being used in building structures. The CFDST beam–columns were found to have significant increase in strength, ductility, and dissipated energy over the outer jackets.

In general, the ductility and energy dissipation ability of specimens with circular sections are higher than those of the specimens with square sections. The mechanics model which was developed by the authors for concrete filled steel tubular (CFST) beam–columns subjected to constant axial load and cyclically increasing flexural load is used to analyze the behavior of CFDST beam–columns. It is found that the predicted cyclic responses for the composite beam–columns are generally in reasonable agreement with test results (Han, Huang, Tao, & Zhao, 2006).

The following figures show the column details and dimensions of the samples and the schematic view of the test setup.

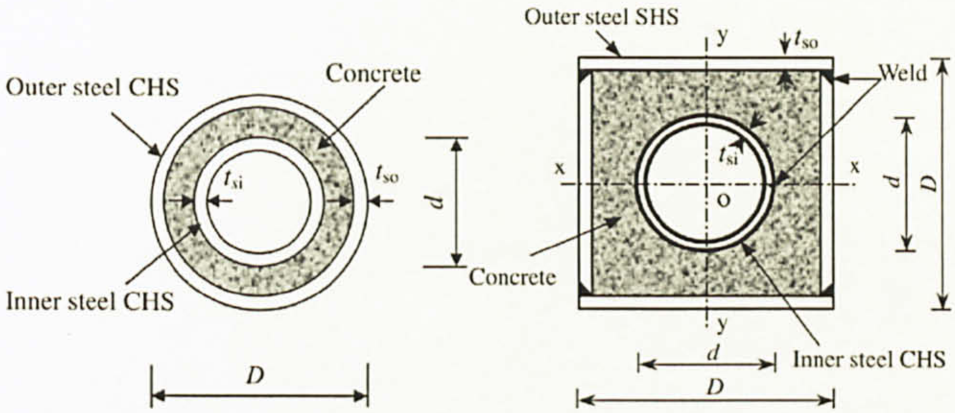

(a) CHS outer and CHS inner. **(b) SHS outer and CHS inner.**

Figure 1.1: Column specimen details and dimensions

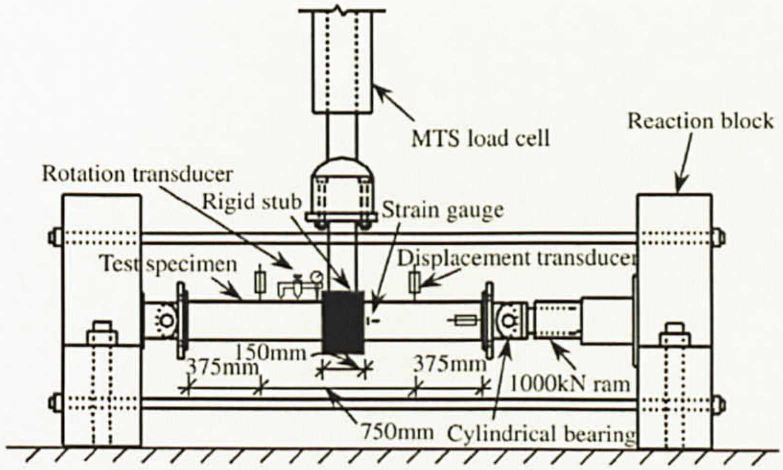

Figure 2.2: Schematic view of the test setup and the arrangement of measuring devices

In this study, CFDST beam–columns exhibit very high levels of energy dissipation and ductility even under high axial load levels. Generally, the energy dissipation ability of the beam–columns with circular sections was much higher than those of the specimens with square sections. It was found that, in general, the mechanics model developed for fully concrete filled steel tubes (CFST) is acceptable for the analysis of CFDST beam–columns, i.e. the predicted lateral load versus lateral deflection curves for CFDST specimens have been found in reasonable agreement with experimental ones.

2.7 Energy Absorption Capacity of Composite Beams

Local buckling may occur in the compression flange of rectangular hollow-section beams under cyclic repeated load arising from earthquakes. Once a local mechanism forms, residual strength rapidly reduces within a few cycles. This is true even for compact sections under static bending.

Concrete-filled steel tubes (CFSTs) are used in many structural applications including columns, supporting platforms of offshore structures, roofs of storage tanks, bridge piers, piles, and columns in seismic zones (Kilpatrick & Rangan, 1995). Concrete-filled steel box columns offer excellent structural performance, such as high strength, high ductility and large energy absorption capacity and have been widely used as primary axial load carrying members in high-rise buildings, bridges and offshore structures (Lu & Kennedy, 1994). Application of the CFST concept can lead to overall savings of steel in comparison with conventional structural steel systems.

In CFST composite construction steel tubes are also used as permanent formwork and to provide well-distributed reinforcement (Assi, Qudeimat, & Huniti, 2003; Furlong, 1968). Test results have shown that the concrete core delays local buckling and forces the steel tube to buckle outwards rather than inwards, resulting in a higher flexural strength therefore, tubes with thinner walls could reach yield strength before local buckling occurs (Zhao & Grzebieta, 1999; Lu & Kennedy, 1994). Furlong (1967) reported that using expansive cement enhances the bond and provides chemically prestressed elements and the steel tube is axially loaded the confinement effect is delayed until the expansion of concrete overcomes that of the tube.

The composite action and bond in CFST were also studied by Hunaiti (1997) from this study following interesting findings are observed under axial compression, the steel tube confines the concrete which improves both the axial load resistance and ductility of the CFST members. Different researchers concluded that confinement effectiveness is reduced by using rectangular or square tubes, by using high strength concrete by increasing the slenderness of columns and pure flexural members (Furlong, 1968; Lu & Kennedy, 1994; Kilpatrick & Rangan, 1995). Concrete in-filled beams give additional stiffness, which delays the failure of the columns (Angeline Prabhavathy & Samuel Knight, 2006).

Two failure modes were developed and observed, namely a single outward folding mechanism without cracks (hollow sections) and no folding mechanism was formed only top distortion (filled sections). The type of mechanism depends on the properties of the filler material. Besides, void filling increases energy absorption capacity, reduces the stiffness degradation and increases the ductility factor (Arivalagan & Kandasamy, 2009).

2.8 Design Calculations on Concrete-Filled Thin-Walled Steel Tubes Subjected to Axially Local Compression

The overall strength of the concrete-filled thin-walled steel tubes when subjected to axially local compression depends on the parameters such as the sectional type, local compression area ratio, steel ratio, strength of steel and concrete, and endplate thickness on sectional capacities. The influences of these parameters on the sectional capacities of CFST columns subjected to axially compression have been studied and from the parametric studies, formulas for the calculation of the sectional capacity of CFST columns have also been developed.

2.8.1 Local Compression Area Ratio

The local compression area ratio is inversely proportional to the stiffness and the sectional capacity of the member where the descending brand of the load-deformation curve is also steeper. Under the same local compression area ratio, the deformation corresponding to the circular section is larger than that of square section. This means that the confinement effect of steel tube with circular section is more effective compared to the square steel tube (Han et al. 2008b).

2.8.2 Steel Ratio

The steel ratio is directly proportional to the sectional capacity of the CFST columns and the descending branch of the load-deformation curve is gentler with the increase of the steel ratio. Comparison is made between the sectional capacity of both plain concrete columns and CFST columns under axially compression load. The CFST columns are generally having greater sectional capacity compared to the plain concrete columns due to the higher yield strength of the steel in the CFST columns than that of the yield strength of the plain concrete. However, the steel ratio has less significance influence on the stiffness of the columns.

2.8.3 Steel Yielding Strength

Generally, the sectional capacities of both circular and square sections of CFST columns increase with the increase of the steel yielding strength although the effect of the steel yielding strength is less significance on the stiffness of the member.

2.8.4 Concrete Strength

The load-deformation curves indicate that the concrete strength is directly proportional to the stiffness and results in greater sectional capacity for both circular and square CFST columns.

2.8.5 Endplate Rigidity

The thickness of the endplate has the same effect on the stiffness of the CFST columns as the concrete strength where the thicker the endplate, the greater the stiffness and the sectional capacity of the members.

CHAPTER 3

METHODOLOGY

3.1 Introduction

Hollow sections are used in bridge piers and may be subjected to damage by corrosion or fatigue failure. Sometimes the usage of hollow sections changes thus affecting the load and structure. In this case we can compare the performances of the circular hollow section and rectangular hollow section. The necessary retrofit means is strengthening the tubular member. The two extreme loads may be flexural load and cyclic load. In this study, the flexural behavior and the effect of cyclic load on the GFST beams are studied. The methodology of the study is explained in the segment below.

3.2 Codes and Standards Used For Analysis

This project involves the analysis of the failure modes such as fatigue failure and flexural failure. Thus, certain codes and standards as follows would be referred:

a) Eurocode 4: Design of composite steel and concrete structures
b) BS 5950: Structural use of steelwork in building

Besides, there are equations which derived from journals and related to the analysis of the moment capacity of grout-filled steel beam. The equations would be further verified to determine the validity and the analysis results obtained by using different equations would be compared to each other.

3.3 Materials

Materials used in this project are as follows:

1. 30 circular hollow beams of 1.2m length.
2. 20 circular hollow beams of 0.6m length.
3. Sika Grout-215 with capacity of 75Mpa.

3.4 Test Methodology and Procedures

Laboratory experiments would be conducted to determine the moment capacity of both bare steel beams and grout-filled steel beams. The behavior of grout-filled steel beams under the influence of the cyclic loading would then be observed. There are few main steps needed and are summarized as following:

3.4.1 Selection of Beams

In this project, one of the objectives is to determine the influences of few parameters such as D/t and stiffness of the beams on the capacity of the grout-filled steel beam under flexural cyclic load. Therefore, these are the factors to be considered when selecting and purchasing the samples.

3.4.2 Grout Preparation

Types of grout to be filled into the steel beams would be the "pumpable, non-shrink leveling, premixed cementitious grout with extended working time to suit local ambient temperature" with the compressive strength of 75Mpa. This type of grout would only need the addition of sufficient amount of water to achieve the desired cementitious properties. The details of the grout can be referred to the appendix.

3.4.3 Grout Casting

Grout would be mixed proportionally with water and poured into the steel beams after mixed thoroughly in the mixer according to the instruction of the manual. Besides, the grout would be filled also into the mould to form grout cubes for compression testing to obtain the average capacity of the grout.

3.4.4 Grout-Filled Beams and Bare Steel Beams Preparation

Procedures

1) Steel sections are measured and cut according to the desired sizes with abrasive machine.

2) Grout is mixed proportionally in the mixer according to the manual instruction. To achieve the pourable ratio, 25kg of grout is mixed with 4 litres of water.

3) Grout is filled into five 100mm x 100mm mould to obtain the srength of the grout.

4) To prevent water loss and also flowing of mixed grout from the tubes, the bottom of the tubes are sealed with clay and samples are placed on the tray. Grout is then being poured into the tubes using the proper tool and funnel.

.

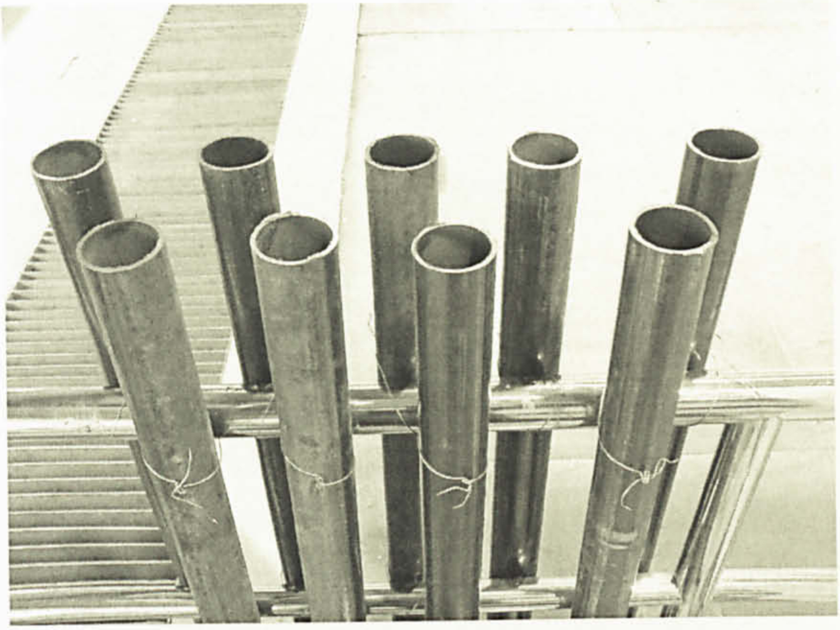

a) Bare steel tubes are tied and to be filled with grout.

b) Bottom of the steel tubes are sealed with clay.

c) Sika grout 215 is mixing in the mixer.

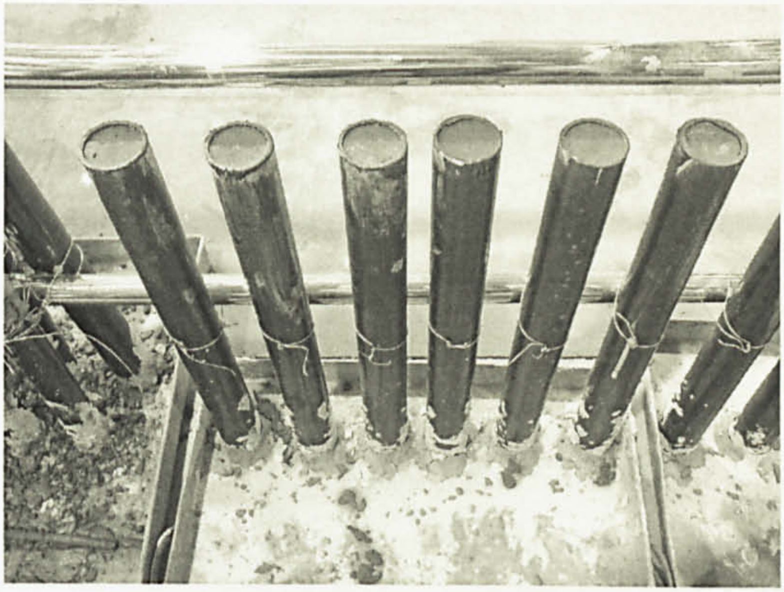

d) Grout casting into steel tubes.

Figure 3.1: Grout-filled beams and bare steel beams preparation

A total of 24 steel beams are prepared for the laboratory work. Among the 24 steel beams, 12 of them are filled with sika grout- 215 and the remaining 12 are prepared as hollow sections. There are two different thickness of beams used which are the 5mm and 3mm with the diameter of 60mm. Besides, the steel beams have been cut into two different lengths which are the 1200mm and 600mm of beams for the comparison of the overall capacity. The steel beams used in this project have Py = 275 N/mm^2 and are classified as high strength steel. The details of the prepared samples are summarized in the following Tables:

Table 3.1: Details and testing method of prepared beam samples

No	Length (m)	Diameter (m)	Thickness (m)	Status	Testing Method	Total
1	0.6	0.06	0.003	3x Filled with grout	3 - Static load	6
				3x Bare	3 - Static load	
2	1.2	0.06	0.003	6x Filled with grout	3 - Static load	12
					3 - Dynamic load	
				6x Bare	3 - Static load	
					3 - Dynamic load	
3	1.2	0.06	0.005	3x Filled with grout	3 - Static load	6
				3x Bare	3 - Static load	

The testing details for the samples would be described in the following sections.

3.4.5 Static Load Testing for the Grout-filled Steel Beams and Bare Steel Beams

The experimental setup used is shown in following figure:

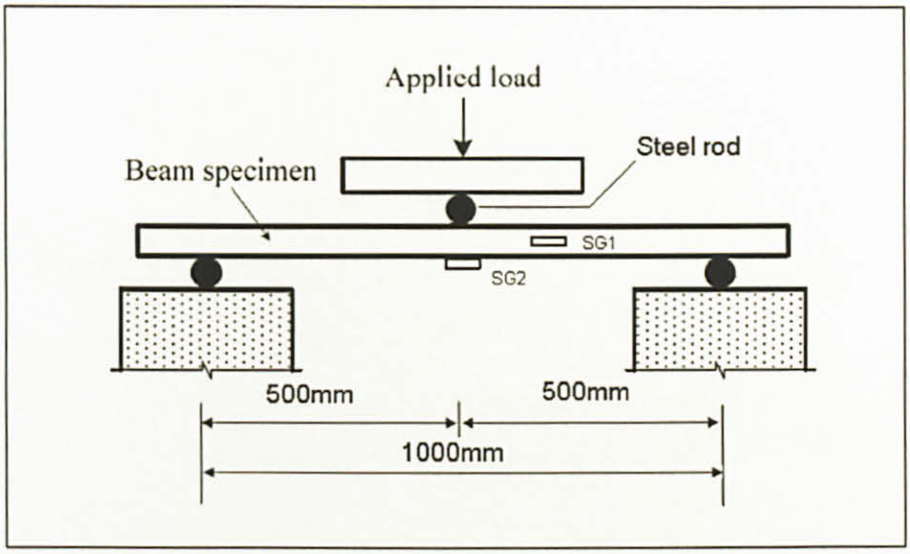

Figure 3.2: Details of static load system for beam specimens

Beam specimens of 1200 mm span length are placed in simply supported by 40mm diameter steel rods. The beams were tested under one point load applied at the centre of a very rigid plate to ensure the load distribution. Two strain gauges were bonded on the specimen, one gauge in the middle and another at the bottom centre of specimen as shown in Figure 5. The strain gauges would be used to determine the maximum compressive and tensile strains. The test specimens were instrumented to measure loads and strains. The beams would be tested under one-point load in a 500kN capacity dynamic machine. The instruments would be controlled and calibrated according to standard specifications. Load interval 0.2kN/s would be used and all specimens would be loaded to failure. The maximum load of each beam specimen would be recorded for the cyclic load testing purposes.

3.4.6 Cyclic Load Testing for the Grout-filled Steel Beams and Bare Steel Beams

The experimental setup used is shown in following figure:

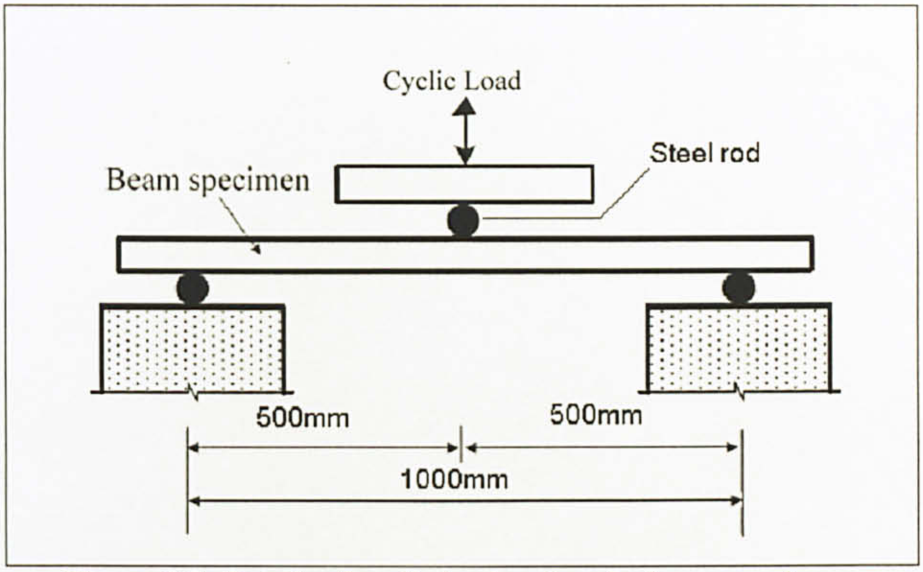

Figure 3.3: Details of cyclic load system for beam specimens

In this cyclic load testing, the same 500kN capacity dynamic machine would be used but without the application of the strain gauges on the samples as shown in Figure 6. The grout-filled steel tube would be first tested to determine its ultimate capacity under the static load testing. The ultimate compression load, Pult would then be fractionally divided for the testing of the grout-filled steel beams, for example, 0.90 Pult, 0.95 Pult, 1.00 Pult, and so on. The samples would be tested under the flexural cyclic load with the specified magnitudes. In this testing, Level A would be the fractional of Pult as mentioned while the level B would be 0.20 Pult for every specimen. The purpose of setting the variation of Level A and Level B is to create a continuously and varying load during the cyclic load testing.

CHAPTER 4

RESULTS AND DISCUSSIONS

4.1 Results and Findings Overview

The results and findings obtained would be tabulated and analyzed using tables and graphs. In this project, it is crucial to determine the compressive strength of the grout besides the capacity of the grout-filled steel beams. It is because the strength of the grout would directly affect the overall strength of the composite beams.

4.2 Section Properties

The properties and the capacities of the circular hollow sections of the steel beams were determined using the BS 5950: Structural use of steelwork in building. Extra details needed are obtained metal supplier. The main properties of the circular hollow sections of the steel beams are tabulated in the following table:

Table 4.1: Section properties of the circular hollow sections

Hollow Sections	**L (mm)**	**D (mm)**	**t (mm)**	**p_y (N/mm^2)**	**Section Classification**
CHS 60mm	1200	60.00	5.0	275	Plastic
CHS 60mm	1200	60.00	3.2	275	Plastic
CHS 60mm	600	60.00	3.2	275	Plastic

According to BS5950 Part 1, the section classification obtained from the steel hollow sections is Class 1 which is categorized as plastic cross-section. A plastic hinge with sufficient rotation capacity to permit redistribution of moments in the structure is developed and can be used for plastic design (Lam et al, 2006). The fundamental assumption in plastic analysis is that the strain in the steel beam is high enough to allow full plastic capacity to develop. Still, it depends on the compactness of the web. At the plastic state, certain effect such as shrinkage, creep and locked-in stresses have not much influenced as the total load is resisted by a total internal assumed stress block.

4.3 Grout Compression Test Result

The grout is filled into five 100mm x 100mm mould in order to achieve the average compressive strength of grout yield from every batch of SikaGrout 215 mixing. After 28 days of air curing, the average compressive strength of the grout cubes is determined with the universal testing machine. The result of the compressive strength at 28 days is tabulated in Table 4.2 as follows:

Table 4.2: Compression result of grout test cubes

	Compressive Strength (N/mm^2)					
Grout Type/ Grout Cubes	**1**	**2**	**3**	**4**	**5**	**Average**
Sika Grout- 215	73.90	81.20	68.60	71.4	78.1	74.64

According to the table, the value of the grout strength adopted for the SikaGrout- 215 is approximately 75Mpa which is the desired value for the experiment.

4.4 Bare Beams and Grout-Filled Steel Beams Subjected to Static Load

The bare beams and grout- filled steel beams were tested with the Dynamic Machine for the static load testing to obtain the maximum capacity. Every group of beams was tested with three samples to obtain the average result of the overall capacity. The average overall capacity for both bare beams and grout- filled steel beams are tabulated in Table 4.3.

Table 4.3: Average result of overall capacity for every group of bare beams and GFST

1) Beam dimension: L = 0.6m, t=3.2 mm

Types of Beams	Maximum Capacity, Pult (kN)			
	1	2	3	Average
Bare Beams	19.54	22.00	24.56	22.03
GFST	52.90	50.65	48.46	50.67

2) Beam dimension: L = 1.2m, t= 3.2mm

Types of Beams	Maximum Capacity, Pult (kN)			
	1	2	3	Average
Bare Beams	11.78	11.28	11.51	11.52
GFST	20.95	22.50	21.70	21.72

3) Beam dimension: L = 1.2m, t= 5.0mm

Types of Beams	Maximum Capacity, Pult (kN)			
	1	2	3	Average
Bare Beams	28.05	27.81	27.59	27.82
GFST	39.60	40.10	39.80	39.83

Based on the result from Table 4.3, beams with the length of 1.2m and thickness 5.0 mm have the highest overall capacity for both bare beams and GFST compare with the other group of beams. This is due to the lower D/t ratio of the beams as the beams have the greatest thickness which is 5.0 mm. The samples with lower D/t value would have greater resistance against the static load due to the higher value of the thin-walled thickness; it would have higher resistance against bending failure. The reason behind this effect is due to the moment of inertia of beam with thickness of 5.0 mm is larger compared to the moment of inertia of beam with thickness of 3.2 mm. For that reason, the ultimate capacity will increase as the moment of inertia is increased where the thickness varies and this contributes to the greater overall capacity. Beams with the length of 1.2m and thickness 3.2mm have the lowest overall capacity for both bare beams and GFST among the beam samples. Although group 2 and group 3 beams have the same thickness which is 3mm, group 3 beams with the length of 0.6m have the greater overall strength due to the shorter length which contributes to the greater stiffness for the beams.

The comparison of experimental result and theoretical data of the bare beams is summarized in the Table 4.4

Table 4.4: Comparison of experimental result and theoretical data of the bare beams

No	Bare Beams, (dia= 60mm)	P_{theory} (kN)	P_{exp} (kN)	% Difference
1	1.2m, t= 5.0mm	14.03	27.82	98.29
2	1.2m, t= 3.2mm	9.53	11.52	20.88
3	0.6m, t=3.2mm	19.07	22.03	15.52

From Table 4.4, the P_{exp} for all the bare beams is higher compare with the P_{theory}. This is because for the calculation of the P_{theory}, the nominal value of the yield strength of the beam and the geometry and thickness of the beam is used. In the laboratory works, the yield strength of the beam and the geometry and thickness of the beam might be different from the nominal value for each sample. Therefore, there is difference between the P_{exp} and P_{theory} for every sample.

According to the Table 4.4, beams with the length of 1.2m and thickness of 5mm have the highest percentage of difference between P_{theory} and P_{exp}. Beams with the shortest length of 0.6m and thickness of 3.2mm have the lowest percentage of difference between P_{theory} and P_{exp}. This beam is categorized as short beam and it is controlled by shear instead of flexural bending. Therefore, the confinement effect of the beam is greater in this case. For the next section which is the percentage of increment of the overall strength for grout- filled steel beams compare with bare beams, the results is summarized in Table 4.5.

Table 4.5: Percentage of increment of the overall strength for grout- filled steel beams compare with bare beams

No	Beam Samples, (dia=60mm)	Maximum Capacity P (kN)		% Increment
		Bare Beams	GFST	
1	1.2m, t= 5.0mm	27.82	39.83	43.17
2	1.2m, t= 3.2mm	11.52	21.72	88.54
3	0.6m, t=3.2mm	22.03	50.67	130.00

The percentage of increment of the overall strength for GFST compare with the bare beams is significant for all groups of beam samples which range from 40% to 130%. The increase in the overall strength is caused by the steel and concrete that acts together where the steel will be in tension while the concrete in compression. The steel section will confine the core concrete from volume increase caused by the cracks and thus increasing the ultimate capacity.

4.5 Bare Beams and Grout-Filled Steel Beams Subjected to Flexural Cyclic Load

The type of cyclic stresses applied on structural systems and the terminologies are illustrated in Figure 4.1.

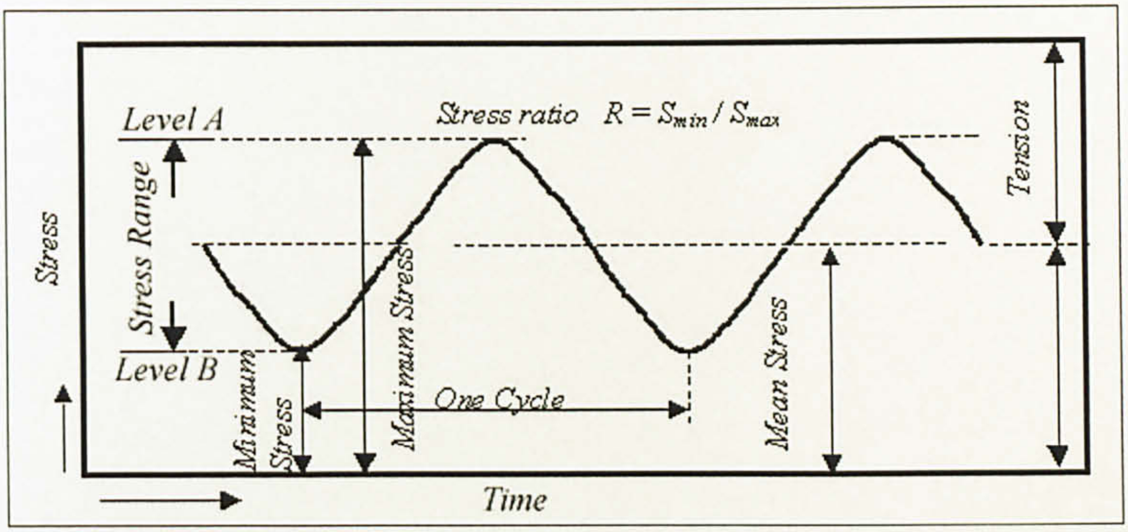

Figure 4.1: Terminology used in fatigue resistant design of structural steel work

The bare beams and grout- filled steel beams were tested with the Universal Testing Machine for the flexural cyclic load testing to investigate the behavior of the beams. The frequency of the cyclic load testing has been set to 5.0 Hz and the machine could generate 300 cycles in one minute. For bare beam samples with the length of 1.2m and thickness of 3.2mm, they have been tested with two set of stress range which is the 0.90 Pult/0.2Pult and 0.95Pult/0.2Pult. The particular beams were selected because among the three groups of samples with different dimensions, the beams chosen for the cyclic load testing have the lowest overall capacity. It means the beam samples would have the more significant result if we compare with the other group of beam samples. Therefore, it could be used as the standard for the other cyclic load testing. The details for the bare beam samples tested under cyclic load are summarized in Table 4.6:

Table 4.6: Details of the bare beams tested with flexural cyclic load

Beam dimensions: L = 1.2m, t= 3.2mm

No	Types of Beams	Pult (kN)	Stress Range (kN)		Cycles
			Level A(S_{max})	Level B (S_{min})	
1	Bare Beams	11.53	0.90Pult (10.38)	0.20Pult (2.31)	111000
2			0.95Pult (10.95)	0.20Pult (2.31)	126000

Based on Table 4.6, the ultimate capacity of the bare beams is 11.53kN which was obtained from the static load testing. The magnitudes for level A are the fraction of the ultimate capacity (0.90Pult and 0.95Pult) since in terms of fatigue failure, the beam samples would fail when subjected to a fluctuating stress even with a magnitude which is lower than the value found from the static load testing.

The strength of the stress range for the cyclic testing is increased from 0.90Pult to 0.95Pult for Level A while the magnitude of Level B is maintained with 0.20Pult due to the insignificant result obtained when the bare beam is subjected to the stress range of 0.90Pult/0.20Pult. After 111000 cycles were applied on the beam, fatigue failure did not occur on the bare beam samples. Therefore, the number of cycles has been increased for the higher strength of the stress range which is the 0.95Pult/0.20Pult.

However, flexural failure still did not occur even though the number of cycles has been increased to 126000 cycles as the deflection of the beams is not significant in terms of fatigue failure. Therefore, higher stress range has been applied to grout- filled steel beams as the beams could sustain higher load due to the confinement effect between the infilled grout and the steel tubes which results in greater overall capacity. The details of the GFST beams tested with flexural cyclic load are tabulated in Table 4.7:

Table 4.7: Details of the GFST beams tested with flexural cyclic load

Beam dimension: L = 1.2m, t= 3.2mm

No	Types of Beams	Pult (kN)	Stress Range (kN)		Cycles
			Level A	Level B	
1	GFST	21.73	0.95Pult (20.64)	0.20Pult (4.35)	265000
2			1.00Pult (21.73)	0.20Pult (4.35)	288000
3			1.20 Pult (26.08)	0.20Pult (4.35)	288000

According to Table 4.7, the ultimate capacity of the GFST beams is 21.73kN which was obtained from the static load testing. The magnitudes for Level A are the fraction of the ultimate capacity but they have been increased (0.905Pult, 1.0Pult, and 1.2Pult) since the GFST beams might sustain higher cyclic load. The magnitude for Level B is maintained at 0.20Pult for all the samples.

For the stress range of 0.95Pult/0.20Pult, the GFST did not fail in terms of fatigue failure although the number of cycles has been increased to 265000 cycles compare to the 126000 cycles which is applied on the bare beams with the same stress range as shown in Table 7. The number of cycles applied on the GFST was two times on the bare beams but still, the deflection was not significant in terms of fatigue failure. Therefore, the magnitude of Level A has been increased to 1.00Pult (21.73kN) which is the maximum capacity of the GFST beams and even increased to the magnitude which is higher than the maximum capacity. In this case, the magnitude of Level A applied on the GFST beams was 1.20Pult or 26.08kN. For both cases, the GFST beams did not fail in term of fatigue failure. The effect of the cyclic load on the GFST beams is less significant if comparing to bare beams based on the condition of both bare beams and GFST beams after subjected to cyclic loading. For more details regarding the effect of cyclic loading on both types of beams, refer to Appendix C.

4.6 S-N Curves and Fatigue Resistant

The common form of presentation of fatigue data is by using the S-N curve, where the stress range (S) is plotted against the number of cycles to failure (N) in logarithmic scale. A typical S-N curve is shown in Figure 4.2.

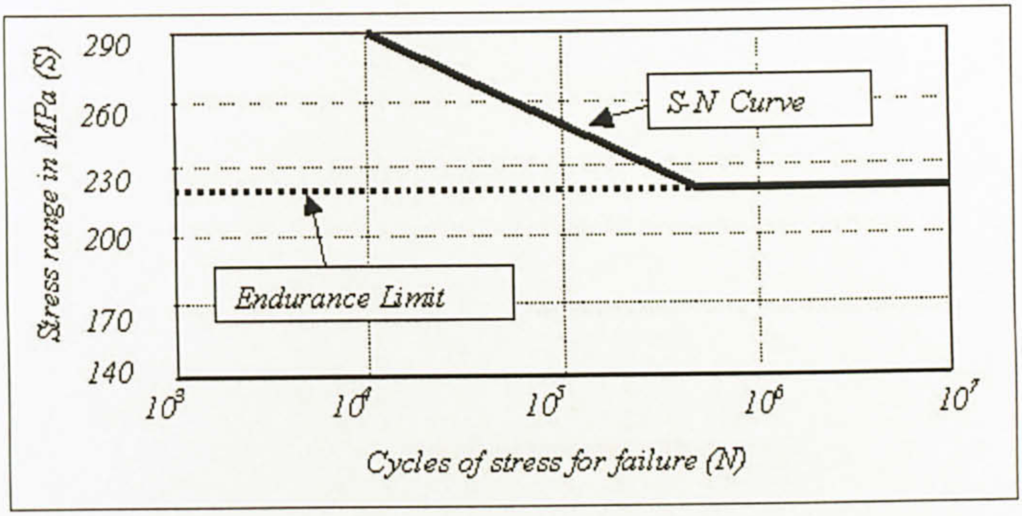

Figure 4.2: S-N diagram for fatigue life assessment

It is seen from Figure 4.2 that the fatigue life reduces with respect to increase in stress range and at a limiting value of stress, the curve flattens off. The point at which the S-N curve flattens off is called the 'endurance limit'. To carry out fatigue life predictions, a linear fatigue damage model is used in conjunction with the relevant S-N curve. The relation between stress and the number of cycles for failure could be written as:

$$\log N = \log C - m \log S$$

where

N - the number of cycles to failure

C - the constant dependant on detailing category

S - the applied constant amplitude stress range

m - the slope of the S-N curve.

For the purpose of design it is more convenient to have the maximum and minimum stresses for a given life as the main parameters. The maximum stresses are plotted in the vertical ordinate and minimum stresses as abscissa. Different curves for different values of fatigue life 'N' can be drawn through point 'C' representing the fatigue strength for various numbers of cycles.

For this project, the constant, C is unknown for the GFST beams as the relationship between the steel and the infilled grout is complicated. Extensive research should be done to determine the constant, C for GFST beams. Therefore, it would have difficulty in comparing the theoretical value and the laboratory result both results. However from figure 4.2, the relationship between the stress range and the number of cycles is clearly defined and this is important for the further research works.

4.7 Fatigue of Bare Beams and Grout- Filled Steel Beams

Generally, the fatigue failure is due to progressive propagation of flaws in steel under cyclic loading. This is partially enhanced by the stress concentration at the tip of such flaw or crack. As we can see from Figure 4.3, the presence of a hole in a plate or simply the presence of a notch in the plate has created stress concentrations at the points 'm' and 'n'. The stress at these points could be three or more times the average applied stress. These stress concentrations may occur in the material due to some discontinuities in the material itself. These stress concentrations are not serious when a ductile material like steel is subjected to a static load, as the stresses redistribute themselves to other adjacent elements within the structure.

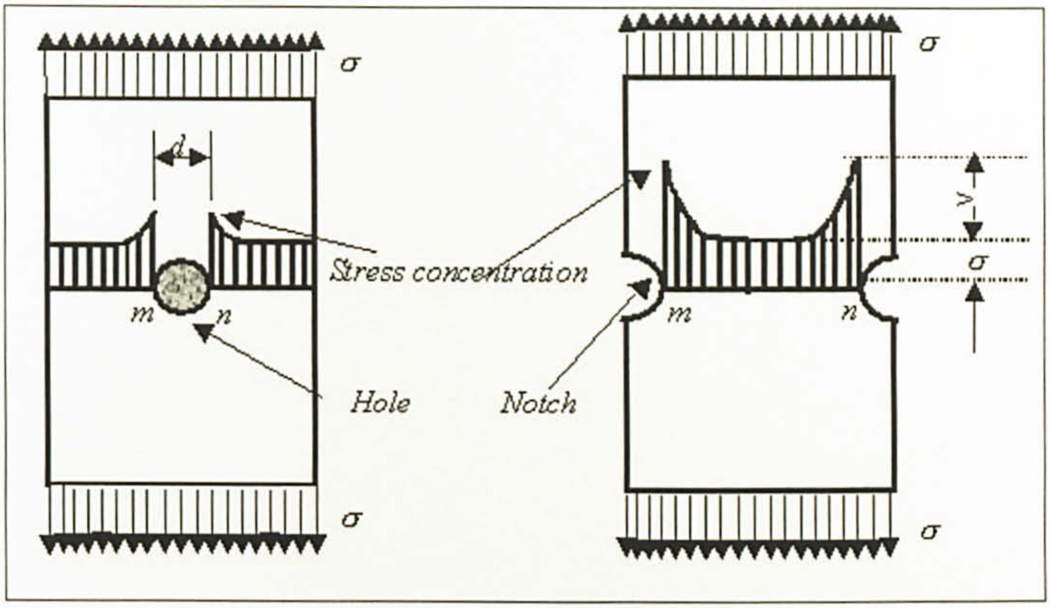

Figure 4.3: Stress concentrations in the presence of notches and holes

At the time of static failure, the average stress across the entire cross section would be the yield stress as shown in Figure 4.3. However when the load is repeatedly applied or the load fluctuates between tension and compression, the points m, n experience a higher range of stress reversal than the applied average stress. These fluctuations involving higher stress ranges, cause minute cracks at these points, which open up progressively and spread with each application of the cyclic load and ultimately lead to rupture.

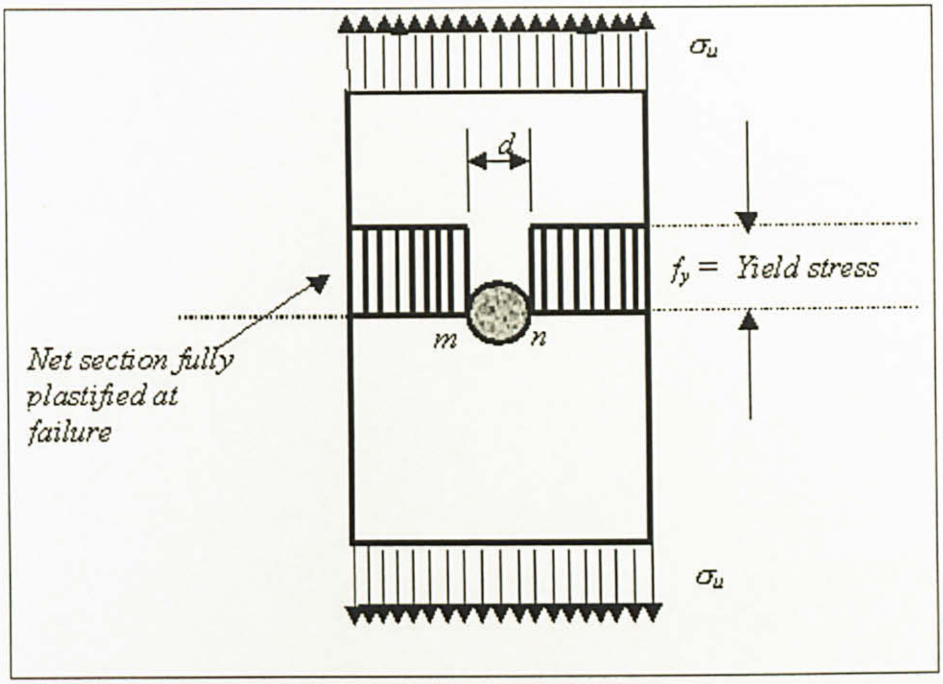

Figure 4.4: Stress pattern at the point of static failure.

In this experiment, both bare beams and GFST beams were tested with cyclic load. Bare beams would be more prone to fatigue failure compare to GFST beams as for the GFST beams, the confinement effect between the infilled grout and the steel beam might yield greater resistance to fatigue failure. Besides the flaws in the beams, there are also several factors which would affect the fatigue failure and would be discussed in the following sections.

4.7.1 Number of cycles in fatigue failure

Fatigue failure can be defined as the number of cycles and hence time taken to reach a pre-defined or a threshold failure criterion. Fatigue failures are classified into two categories namely the high cycle and low cycle fatigue failures, depending upon the number of cycles necessary to create rupture. Low cycle fatigue could be classified as the failures occurring in few cycles to a few tens of thousands of cycles, normally under high stress/ strain ranges. High cycle fatigue requires about several millions of cycles to initiate a failure.

Based on the results obtained from the experiments, the bare steel beams used are classified as high cycles fatigue failure because fatigue failure did not happen on the beams after over hundred thousand cycles have been applied. For the GFST beams used, It might be classified as high cycles fatigue failure based on the results obtained. However, through the observation of the samples after over two hundred thousand cycles with high stress range which is in this case 1.2Pult/0.2Pult have been applied, the effect of the cyclic load on the GFST beams is less significant compared to the bare beams with lower number of cycles and stress range. Fatigue failure probably might not happen in the GFST beams used.

4.7.2 Stress range in fatigue failure

The stress range is the important parameter in the fatigue resistant design. Higher the stress range a component is subjected to, lower would be its fatigue life and lower the stress range, higher would be the fatigue life. It becomes very important to avoid any local structural discontinuities and notches by good design and this is the most effective means of increasing fatigue life.

In this case, the stress range has been increased for GFST beams compare to the bare beams. Based on the results obtained, the highest stress range applied on the bare beams was 0.95Pult/0.2Pult while for the GFST beams; the highest stress range that has been applied was 1.2Pult/0.2Pult. Such arrangement has been set due to the GFST beams might sustain cyclic load with higher stress range. This was supported by the results obtained whereby the effect of the cyclic load on the GFST beams was less significant compare to the effect of the cyclic load on the bare beams with the same stress range.

CHAPTER 5

CONCLUSION

In this research, overall capacity of bare beams and GFST beams was first determined by the static load testing. The behavior of the bare beams and GFST has been investigated and observed during the laboratory experiments. Based on the results and discussions in previous chapter, it could be concluded that:

1) The static lateral load capacity of bare beams has been increased significantly when infilling with grout. This is due to the confinement effect of the tubular section to the infilled grout which produced greater overall capacity.

2) The bare beams and GFST beams did not fail in terms of fatigue failure when the cyclic load with specified stress range and number of cycles were applied. For GFST beams, value of maximum stress for cyclic load testing was higher than the ultimate capacity of the GFST beams found from static load testing.

3) The D/t ratio and the span of the beams would directly affect the result of cyclic load testing. For bare beams having the same diameter with different thickness subjected to the static load, the beam with lower D/t ratio would have higher overall strength compare to the beam with higher D/t ratio. While for the GFST beams, greater thickness means the confinement effect of the steel would be increased and thus increases the overall capacity of the beams. The GFST beams when subjected to cyclic load would also exhibit higher capacities due to the effect of D/t ratio and confinement.

4) Fatigue failure was not observed in the samples when subjected to cyclic loads with stress ranges 1) 0.95Pult/0.20Pult for bare beam and 2) 1.20Pult/0.20Pult for GFST beam.

RECOMMENDATIONS

Based on the results and discussion, it is found that the bare steel beams and GFST beams used are classified as high cycles fatigue failure. Moreover, GFST beams could also sustain higher stress range of cyclic load. However, there are some recommendations that could be made for the extensive research regarding the effect of cyclic load on the GFST beams in the future.

1) The beams used for the experiment should be checked thoroughly to ensure they are in the best condition for cyclic load testing as flaws, such as discontinuities of the steel members would affect the ultimate result of the fatigue failure. It is advisable to use non-destructive testing (NDT) method to ensure defect free details.

2) The strength of grout used in the research might affect the overall result as the relationship between the grout and the steel beams is complex. This includes variation of the bonding strength which might directly affect the resistance of the GFST beams to the fatigue failure. Therefore, different types of grout (with different strength) could be used in the future research works.

3) Where a structure is subjected to fatigue, it is important that welded joints are considered carefully. Indeed, weld defects and poor weld details are the major contributors of fatigue failures. Thus, GFST beams with welded connection between members are recommended to be used in the future research to investigate the relationship between the connection of the joints and the effect of the cyclic load.

4) The finite element member (FEM) study could be used to investigate the behavior of the GFST beams when tested with cyclic load as the method is so sophisticated and if it is supported by a comprehensive experimental in the future research, together they would bring a new perspective to the GFST beams.

ECONOMIC BENEFITS

The infilled material used in this project to strengthen the beam is SikaGrout 215 instead of the ordinary concrete. It is due to the advantages of the SikaGrout perceived such as:

a) Easy to mix and apply
b) Good flow characteristics
c) Rapid strength development
d) High ultimate strengths
e) Good pumping properties

Below is the detail of cost of using SikaGrout 215:

Table 5.1: Details of the cost of SikaGrout 215

Type of Grout	Packaging	No. of bags used	Volume/bag (litres)	Total Volume (litres)	Cost/ bag (RM)	Total Cost (RM)
SikaGrout 215	25 kg/bag	7	13.2	92.4	28	**196**

Although the cost of using SikaGrout is higher than using concrete as the infilled material, it would be considered cost effective by using SikaGrout if it is to produce in bulk. Besides, based on the advantages of SikaGrout over the ordinary concrete, it is wise and advisable to use this material in structures prone to heavy vibration such as offshore structures and bridges.

REFERENCES

Angeline Prabhavathy, R., & Samuel Knight, G. M. (2006). Behaviour of Cold-Formed Steel Concrete Infilled RH Connections and Frames. *Steel and Composite Structures, , 6* (1), 71-85.

Arivalagan, & Kandasamy. (2009). Energy Absorption Capacity of Composite Beams. *Journal of Engineering Science and Technology Review* , 145-150.

Assi, I. M., Qudeimat, E. M., & Huniti, Y. M. (2003). Ultimate Moment Capacity of Foamed and Flyash Aggregate Concrete-Filled Steel Tubes. *Steel and Composite Structures , 3* (3), 199-212.

Deng, J., & Lee, M. K. (2007). Composite Structures 78. In *Behaviour Under Static Loading of Metallic Beams Reinforced With a Bonded CFRP Plate* (pp. 232-242).

EN1994-1-1. (1994). *Eurocode 4, Design of composite steel and concrete structures, Part 1-1: General rules.* Brussels.

EN1994-2. (1994). *Eurocode 4, Design of composite steel and concrete structures, Part 2: General rules and rules for bridges.* Brussels.

Furlong, R. W. (1968). Strength of steel encased concrete beam-columns. *Journal of Structural Engineering Division, , 94* (ST1), 267-281.

Gho, M. W., & Liu, D. (2003). *Flexural Behaviour of High-Strength Rectangular Concret- Filled Steel Hollow Sections .*

Han, L. H., Huang, H., Tao, Z., & Zhao, X. L. (2006, May 3). Concrete-Filled Double Skin Steel Tubular (CFDST) Beam-Columns Subjected to Cyclic Bending. *Engineering Structures 28* , 1698–1714.

Hanswille, G., Porsch, M., & Ustundag, C. (2007). Resistance of Headed Studs subjected to Fatigue Loading, Part I & Part II: Experimental Study. *Journal of Constructional Steel Research , 63* (4), 475-493.

Kilpatrick, A. E., & Rangan, B. V. (1995). The influence of bond upon the load-deformation response of high-strength composite columns",. *Proceedings of the 14th Australian Conference on the Mechanics of Structures and Materials,* , (pp. 368-372). Hobart.

Lee, H. K., & Hausmann, L. R. (2004). Composite Structures. *Structural Repair and Strengthening of Damaged Beams With Sprayed FRP , 63* (2), 201-209.

Lu, Y. Q., & Kennedy, D. L. (1994). The flexural behaviour of concrete-filled hollow structural sections. *Canadian Journal of Civil Engg. , 21* (1), 111-130.

Oehlers, D. J. (1990). Deterioration in strength of stud connectors in composite bridge beams. *Journal of Structural Engineering , 116* (12), 3417-3431.

Phares, B. M., Wipf, T. J., Klaiber, F., Abu-Hawash, A., & Lee, Y. S. (2003). Strengthening of Steel Girder Bridges Using FRP. *Proceedings of the 2003 Mid-Continent Transportation Research Symposium, Ames, Iowa, August, 2003.*

Photiou, N. K., Hollaway, L. C., & Chryssanthopoulos, M. K. (2006). Strenthening of an Zrtificially Degraded Steel BEam Utilising a Carbon/Glass Composite System. In *Construction and Building Materials 20* (pp. 11-21).

Schnerch, D., Stanford, K., Sumner, E., & Rizkalla, S. (2005). Bond Behaviour of CFRP Strengthened Steel Bridges and Structures. *Proceedings of International Symposium on Bond Behaviour of FRP in Structures.*

Shawkat, W., Fahmy, W., & Fan, A. (2008). Cracking Patterns and Strength of CFT Beams under Different Moment Gradients. *Composite Structures 84* , 159-166.

Soundararajan, A., & Shanmugasundaram, K. (2008). Flexural Behaviour of Concrete-Filled Steel Hollow Section Beams. *Journal of Civil Engineering and Management* , 107-114.

Zhao, X. L., & Grzebieta, R. H. (1999). Void-Filled SHS Beams Subjected to Large Deformation Cyclic Bending. *Journal of Structural Engineering , 128* (9), 1020-1027.

APPENDICES

APPENDIX A: CALCULATIONS

1) Steel size = 60.3 x 3.2mm CHS

2) Py = 275 N/mm^2

3) Section Classification ε = $(275/py)^{0.5}$

$= (275/275)^{0.5}$

$= 1$

D/t = 18.84 < 40 ε

Therefore section is plastic.

4) Steel Properties:

L = 1.2m

$A_s = 574mm^2$

$S = 10400mm^4$

5) Finding Applied Load

M= py x S = 2860000N.mm

= 2.86kN.m

M = PL/4

P = 4M/L = 9.53 kN

Ptheory = 9.53kN

Pexperimental = 11.78kN

1) Steel size = 60.3 x 5.0mm CHS

2) Py $= 275\ N/mm^2$

3) Section Classification ε $= (275/py)^{0.5}$

$= (275/275)^{0.5}$

$= 1$

D/t $= 12.06 < 40\ \varepsilon$

Therefore section is plastic.

4) Steel Properties:

$L = 1.2m$

$A_s = 869mm^2$

$S = 15300mm^4$

5) Finding Applied Load

M= py x S = 4207500N.mm

= 4.21kN.m

M = PL/4

P = 4M/L = 14.03kN

Ptheory = 14.03kN

Pexperimental = 28.05kN

1) Steel size = 60.3 x 3.2mm CHS

2) Py = 275 N/mm^2

3) Section Classification ε = $(275/py)^{0.5}$

$= (275/275)^{0.5}$

$= 1$

D/t = $18.84 < 40\ \varepsilon$

Therefore section is plastic.

4) Steel Properties:

L = 0.6m

$A_s = 574mm^2$

$S = 10400mm^4$

5) Finding Applied Load

M= py x S = 2860000N.mm

= 2.86kN.m

M = PL/4

P = 4M/L = 19.07 kN

Ptheory = 19.07kN

Pexperimental = 19.54kN

APPENDIX B: GRAPHS

BATCH 1 RESULTS FOR STATIC LOAD TESTING

1) Bare Beam: Load- deflection curve for 1.2m length, 3.2mm thickness.
   Maximum Capacity = 11.78kN

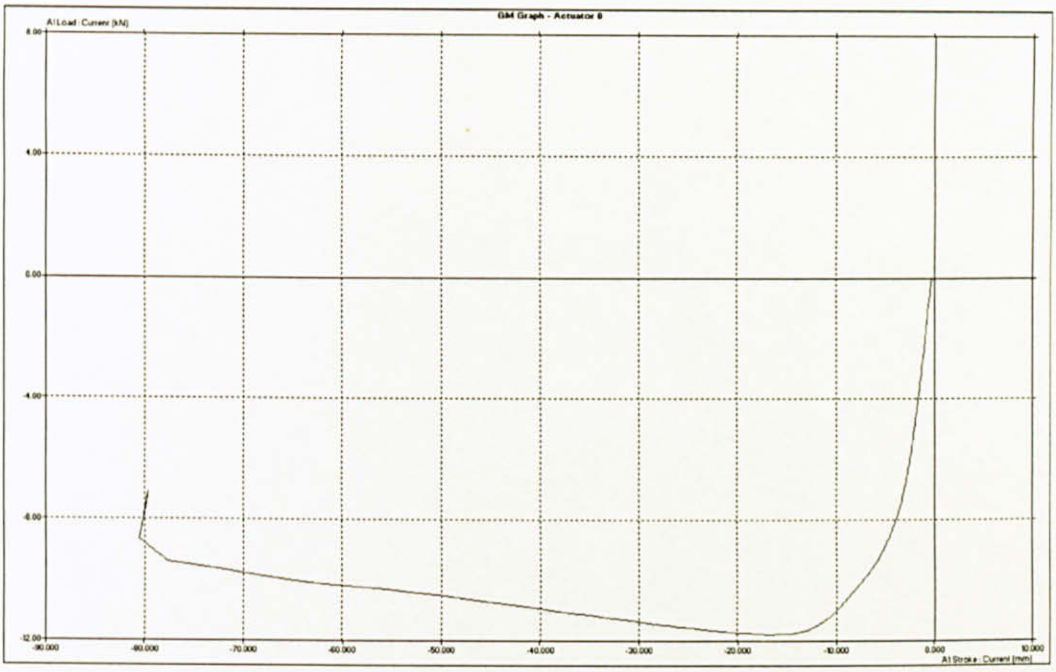

2) GFST Beam: Load- deflection curve for 1.2m length, 3.2mm thickness.
   Maximum Capacity = 20.95kN

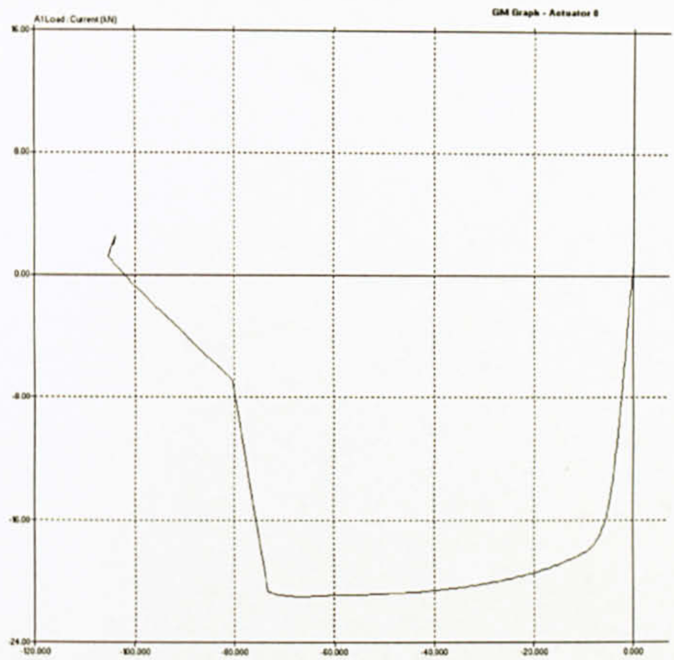

3) Bare Beam: Load- deflection curve for 1.2m length, 5.0mm thickness.
Maximum Capacity =28.05kN

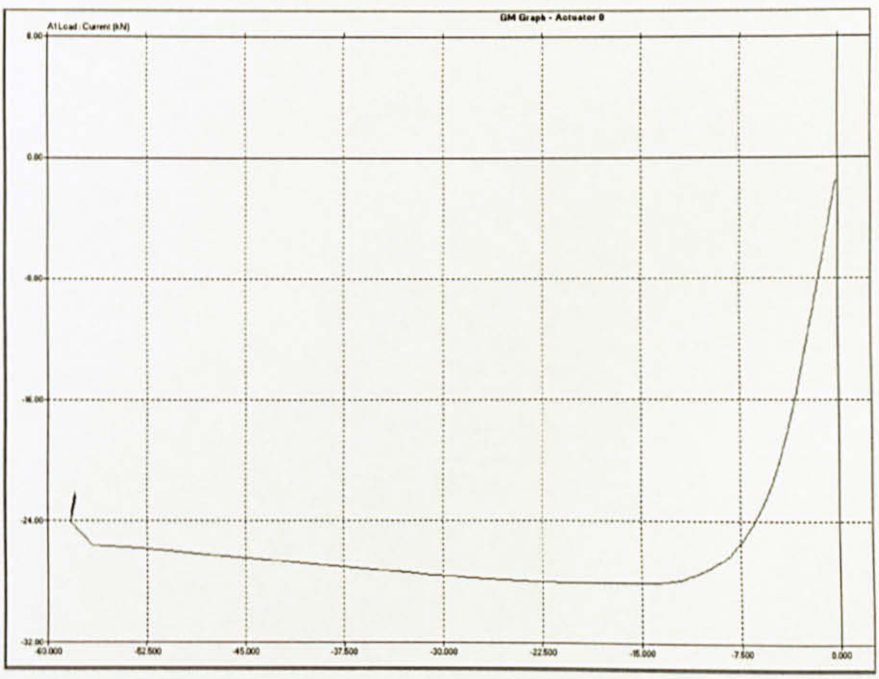

4) GFST Beam: Load- deflection curve for 1.2m length, 5.0mm thickness.
Maximum Capacity = 39.60kN

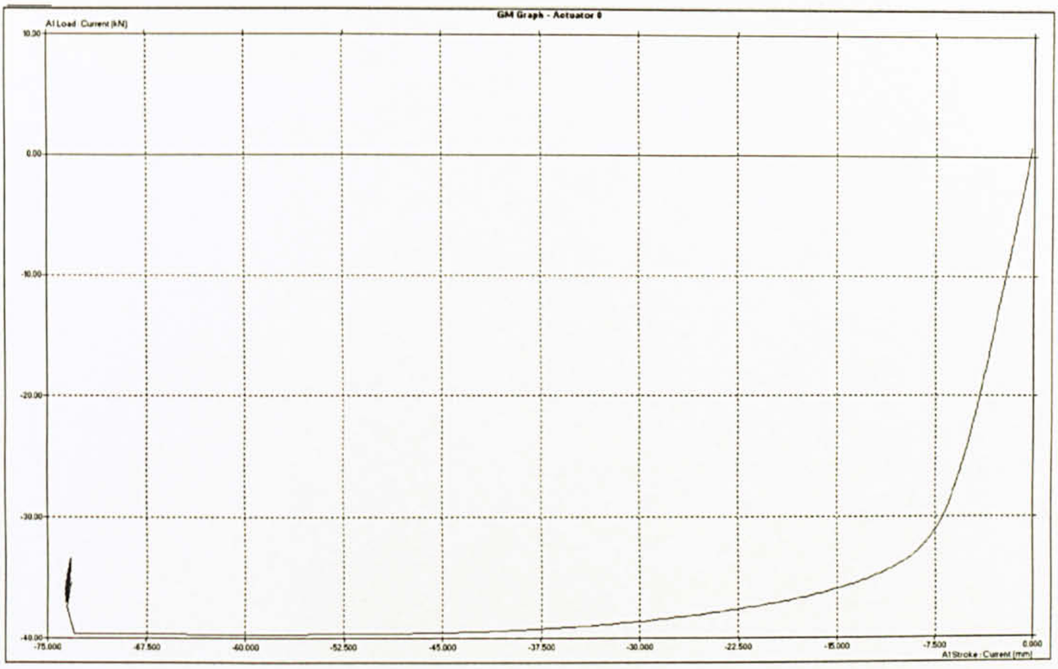

5) Bare Beam: Load- deflection curve for 0.6m length, 3.2mm thickness.
   Maximum Capacity =19.54kN

6) GFST Beam: Load- deflection curve for 0.6m length, 3.2mm thickness.
   Maximum Capacity = 52.90kN

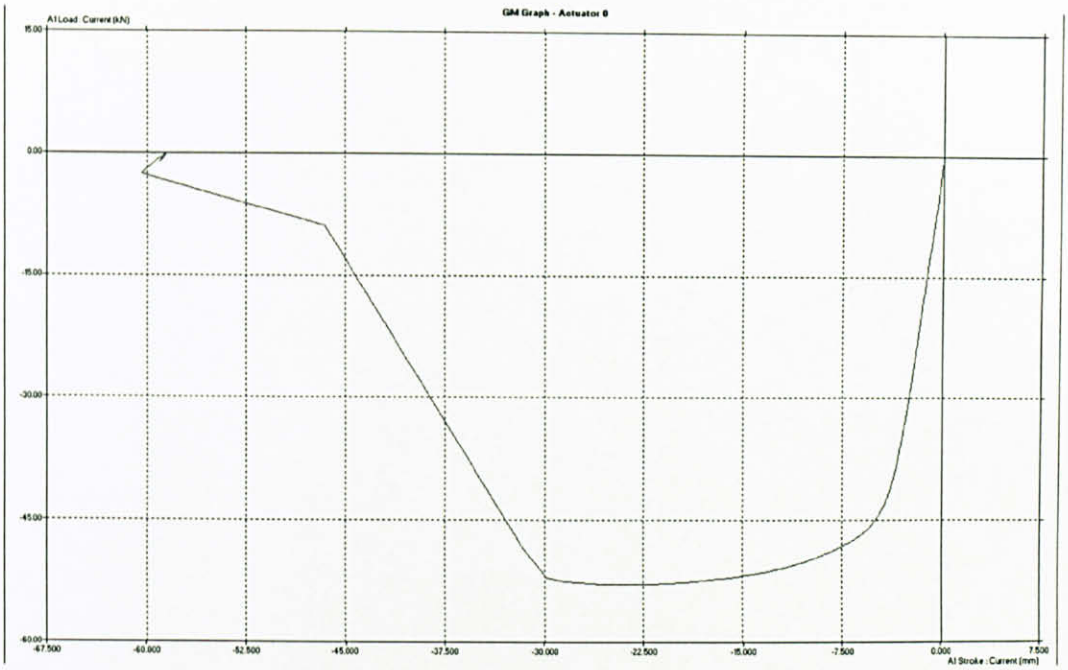
GM Graph - Actuator 0
A1 Load : Current (kN)
15.00
0.00
-15.00
-30.00
-45.00
-60.00
-67.500
-60.000
-52.500
-45.000
-37.500
-30.000
-22.500
-15.000
-7.500
0.000
7.500
A1 Stroke : Current (mm)

BATCH 2 RESULTS FOR STATIC LOAD TESTING

1) Bare Beam: Load- deflection curve for 1.2m length, 3.2mm thickness.
   Maximum Capacity = 11.28kN

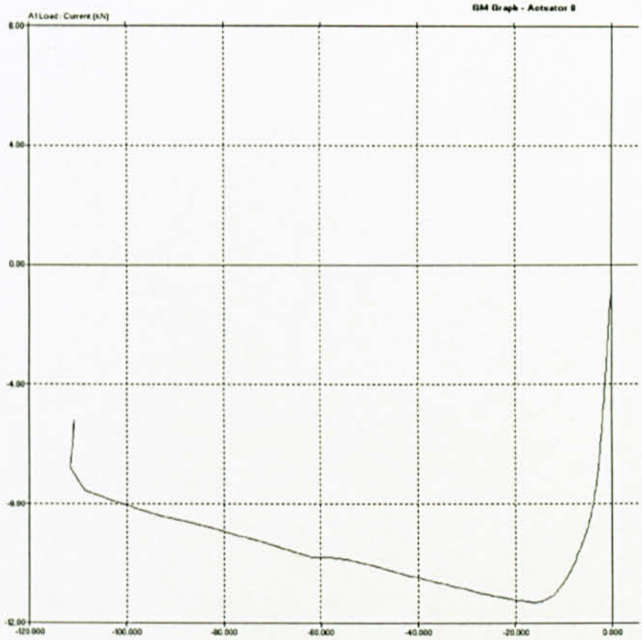

2) GFST Beam: Load- deflection curve for 1.2m length, 3.2mm thickness.
   Maximum Capacity = 22.50kN

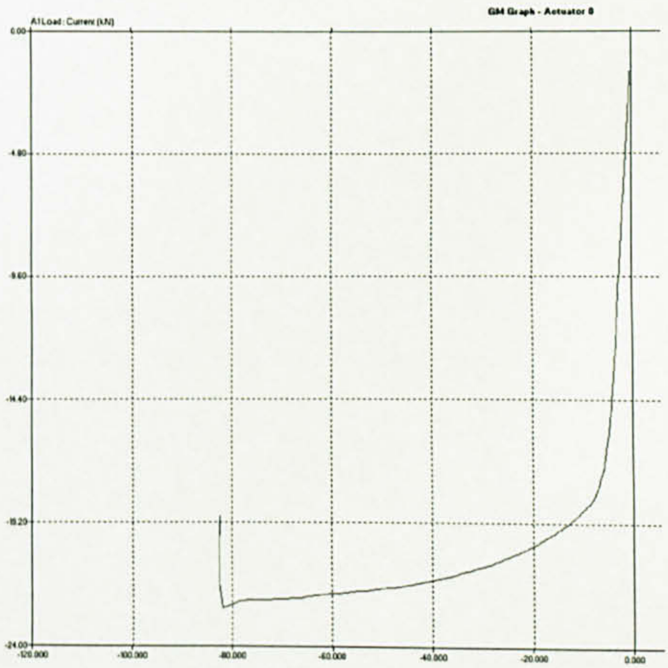

3) Bare Beam: Load- deflection curve for 1.2m length, 5.0mm thickness.
Maximum Capacity = 27.59kN

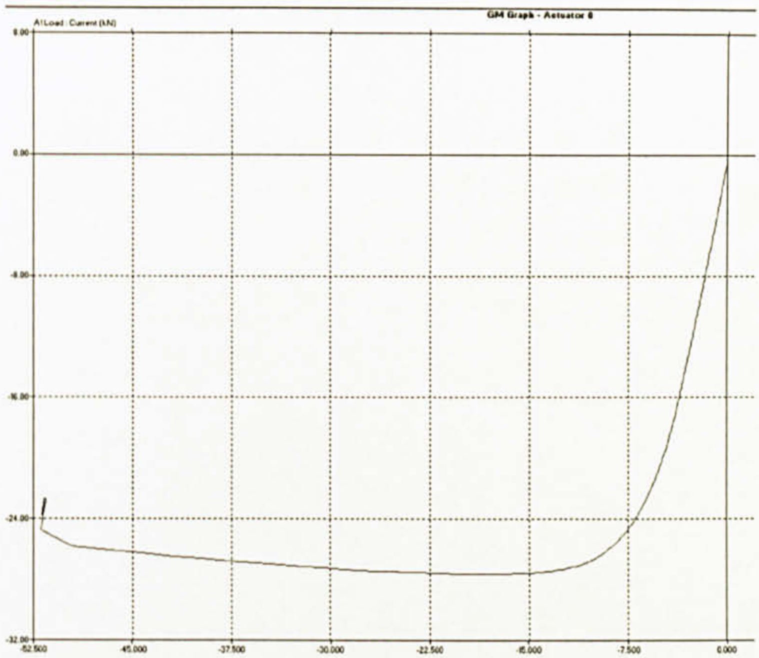

4) GFST Beam: Load- deflection curve for 1.2m length, 3.2mm thickness.
Maximum Capacity = 40.10kN

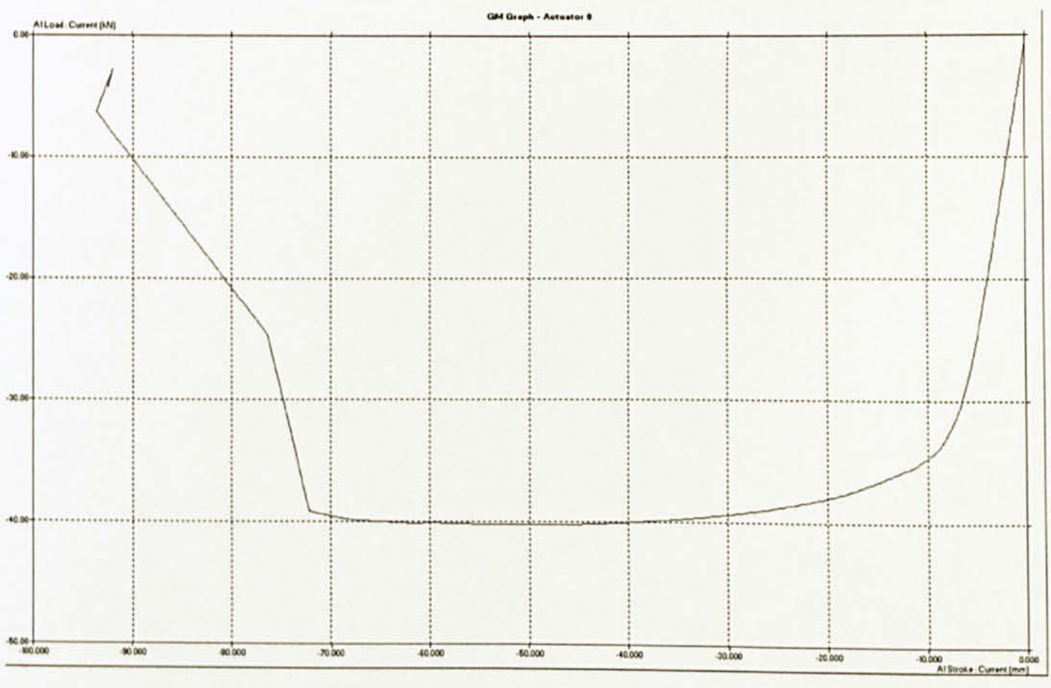

5) Bare Beam: Load- deflection curve for 0.6m length, 3.2 mm thickness.
Maximum Capacity = 24.56kN

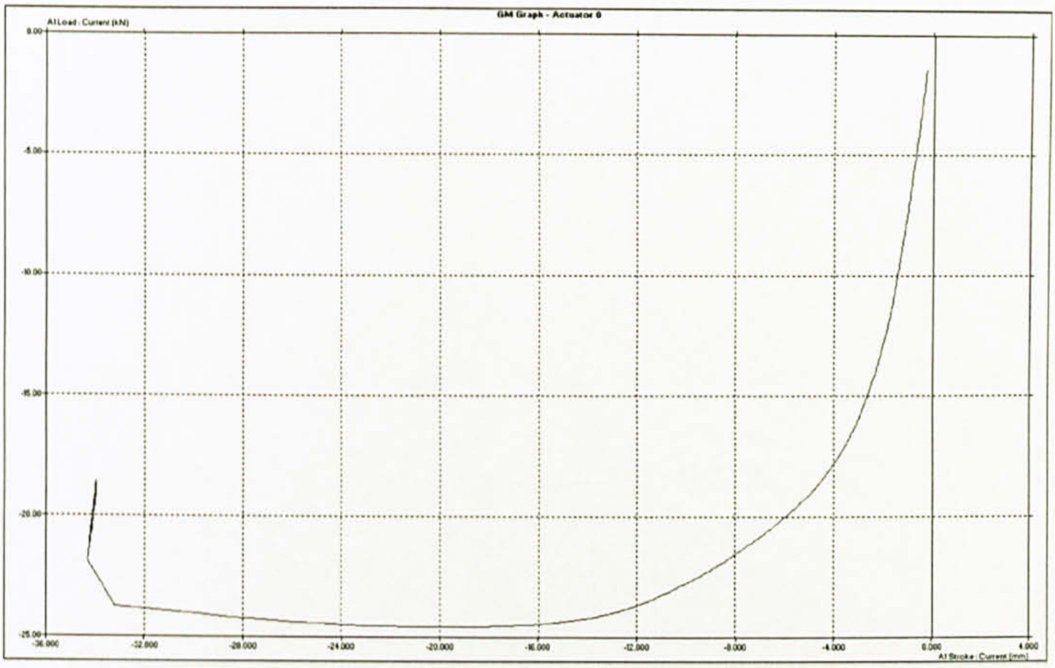

6) GFST Beam: Load- deflection curve for 1.2m length, 3.2mm thickness.
Maximum Capacity = 48.46kN

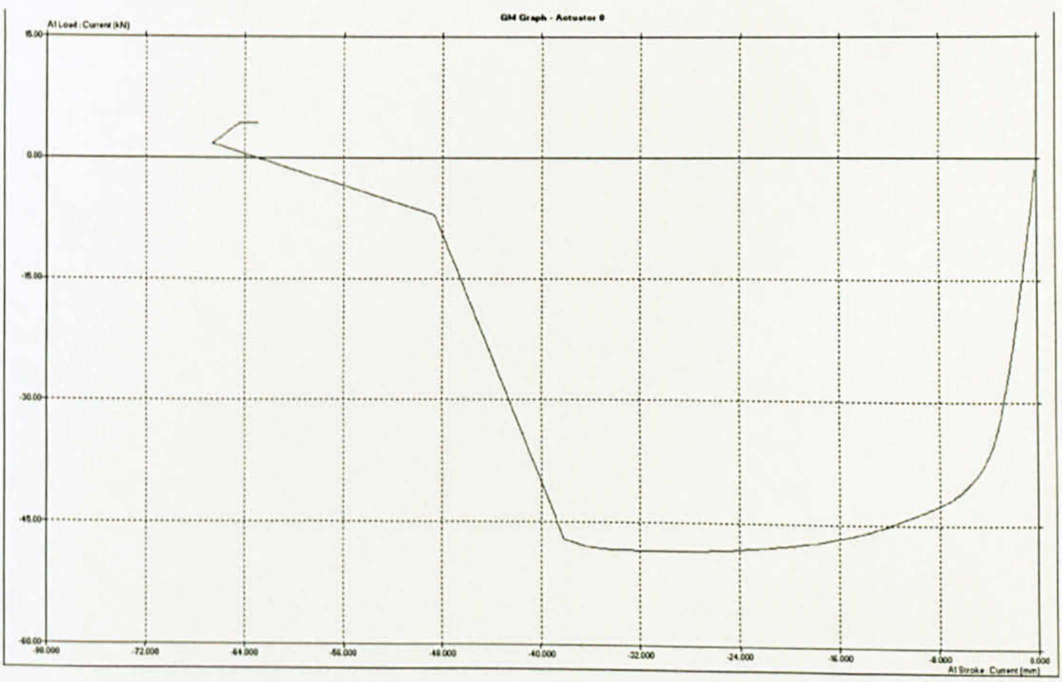

RESULT FOR CYCLIC LOAD TESTING

1) Bare Beam (0.90Pult/0.2Pult): Cyclic load graph for 1.2m length, 3.2mm thickness.
   a) Cycles done = 1000

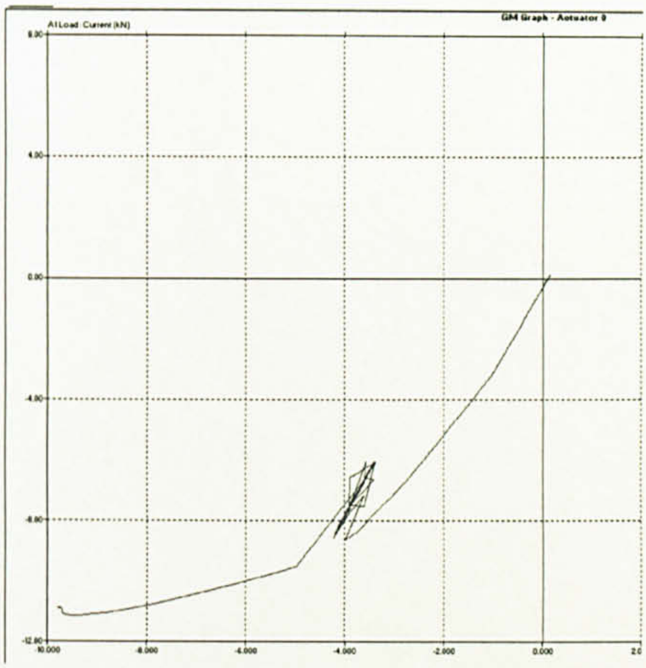

   b) Cycles done = 5000

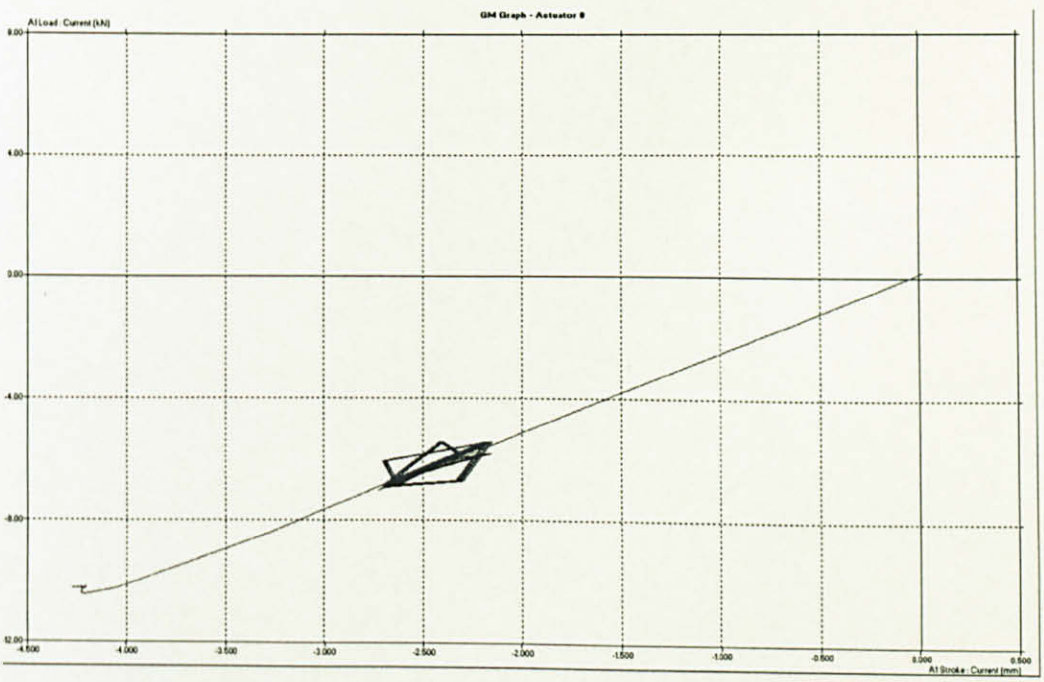

c) Cycles done = 15000

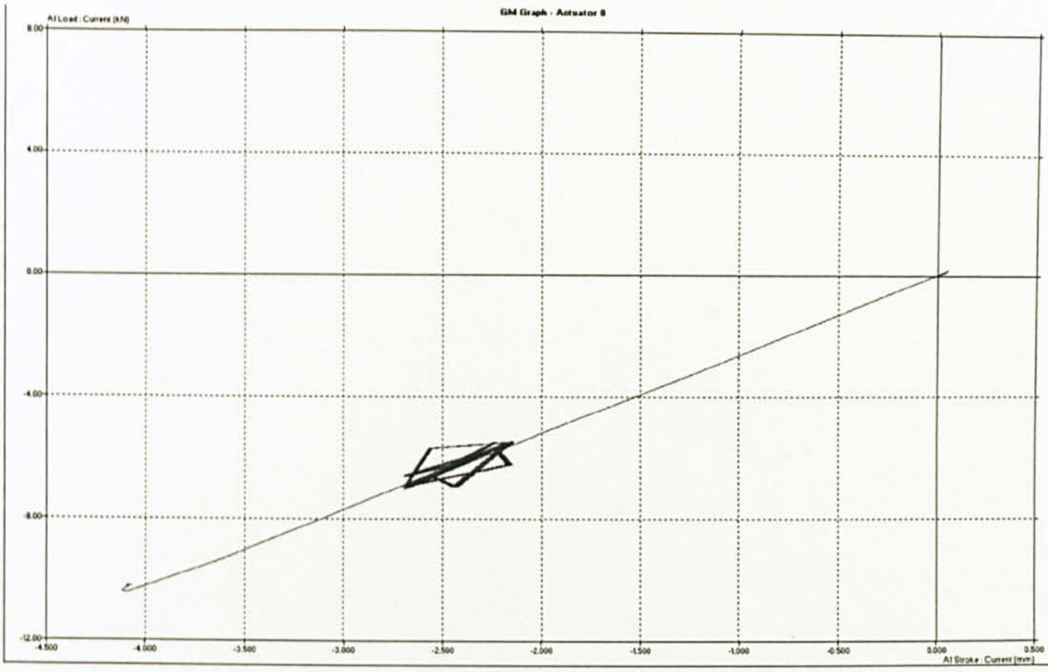

d) Cycles done = 90000

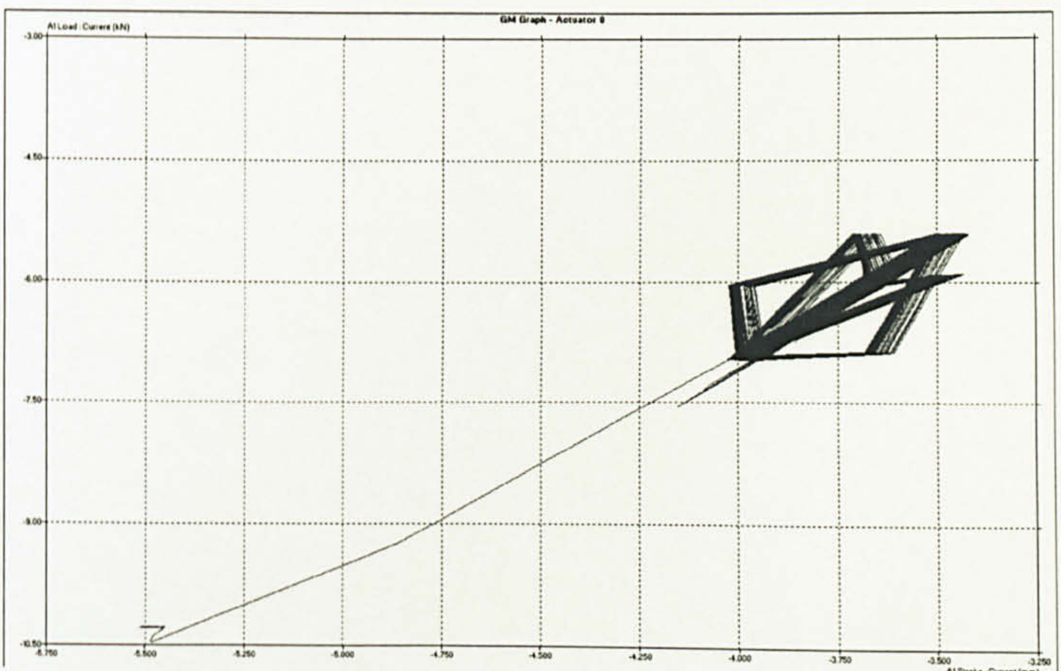

Total cycles done for Bare Beam (0.90Pult/0.2Pult): Cyclic load graph for 1.2m length, 3.2mm thickness = **111000**

2) Bare Beam (0.95Pult/0.2Pult): Cyclic load graph for 1.2m length, 3.2mm thickness
Total Cycles done = **126000**

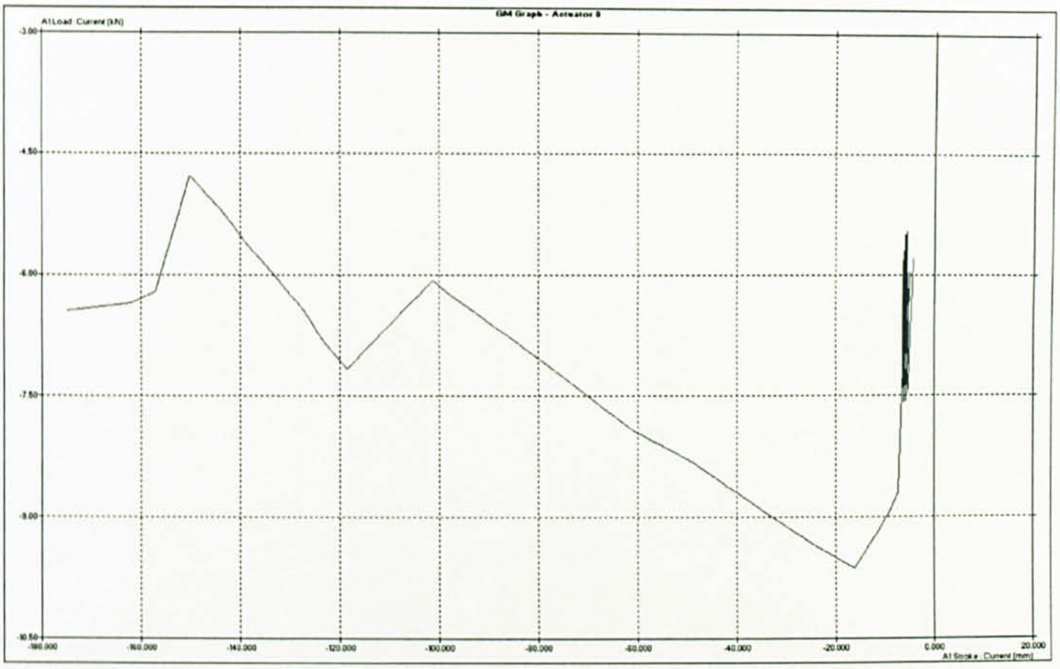

3) GFST Beam (0.95Pult/0.2Pult): Cyclic load graph for 1.2m length, 3.2mm thickness

a) Cycles done = 125000

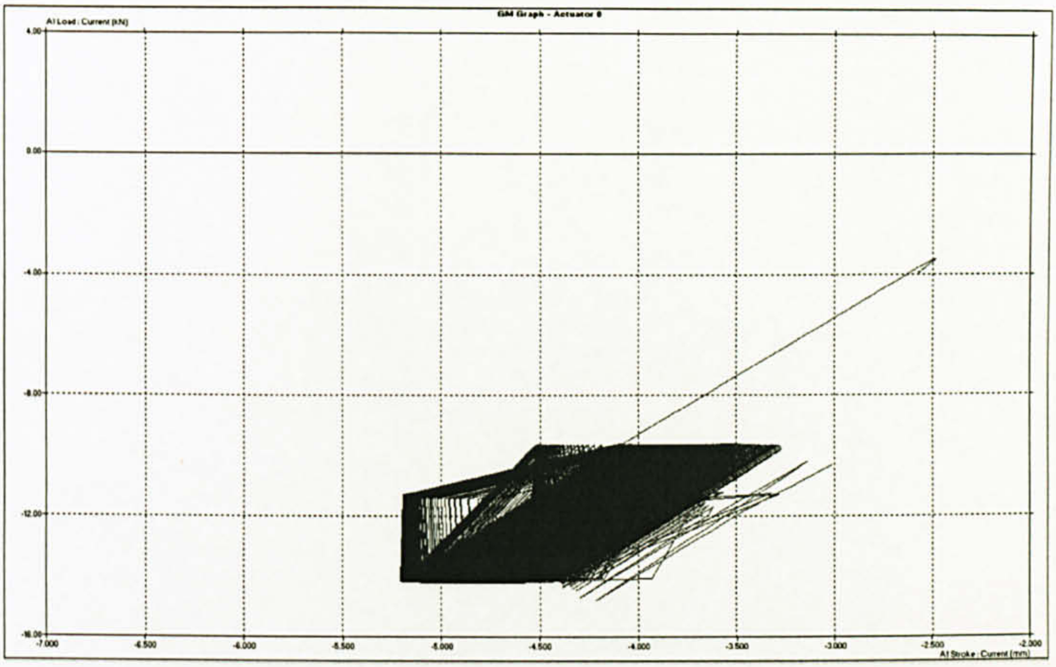

b) Cycles done = 140000

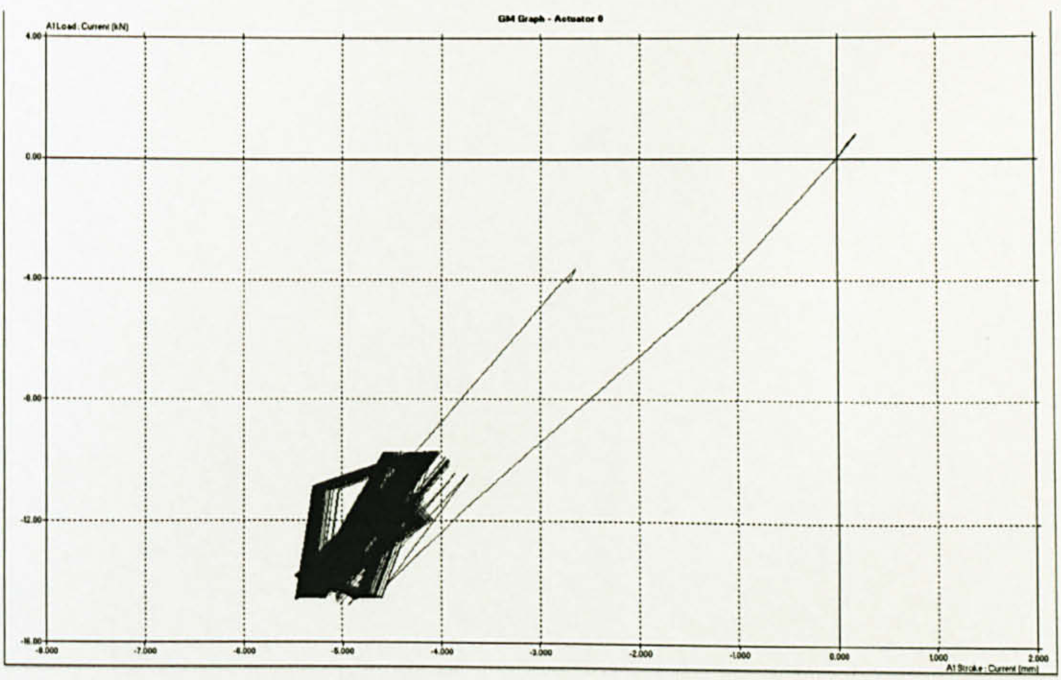

Total cycles done for GFST Beam (0.95Pult/0.2Pult): Cyclic load graph for 1.2m length, 3.2mm thickness = **265000**

4) GFST Beam (1.00Pult/0.2Pult): Cyclic load graph for 1.2m length, 3.2mm thickness

a) Cycles done = 144000

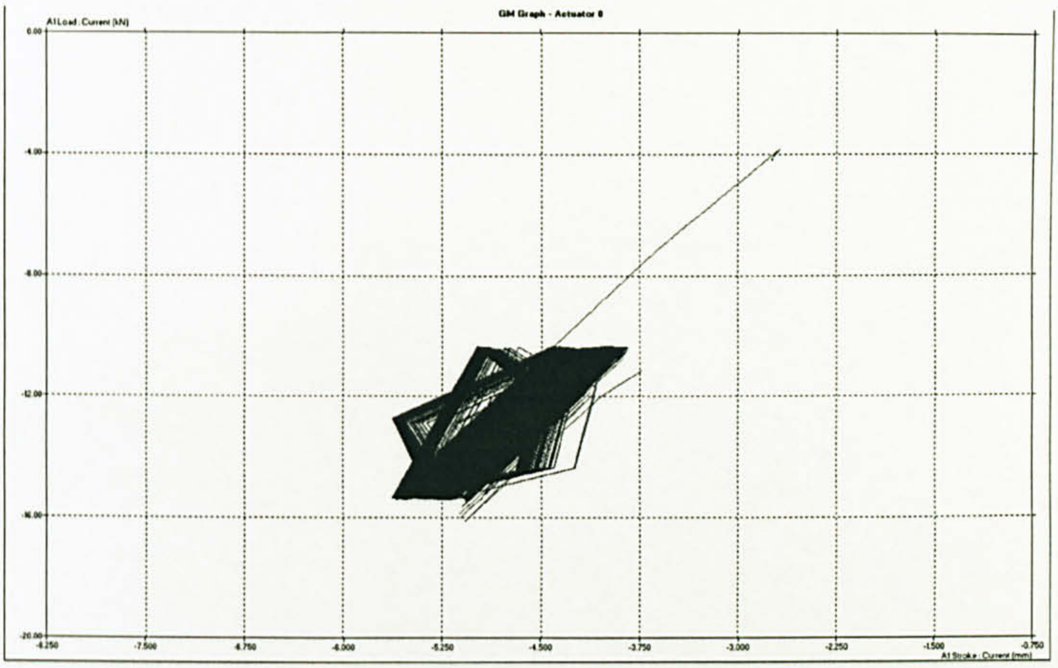

b) Cycles done = 144000

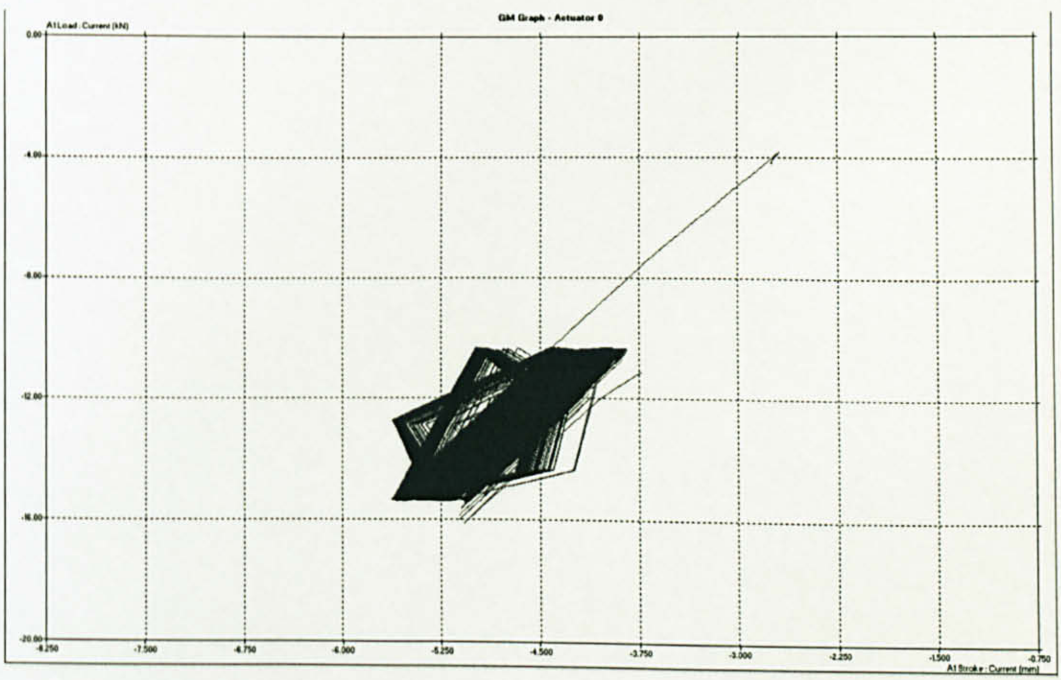

Total cycles done for GFST Beam (1.00Pult/0.2Pult): Cyclic load graph for 1.2m length, 3.2mm thickness = **288000**

5) GFST Beam (1.20Pult/0.2Pult): Cyclic load graph for 1.2m length, 3.2mm thickness
   a) Cycles done = 144000

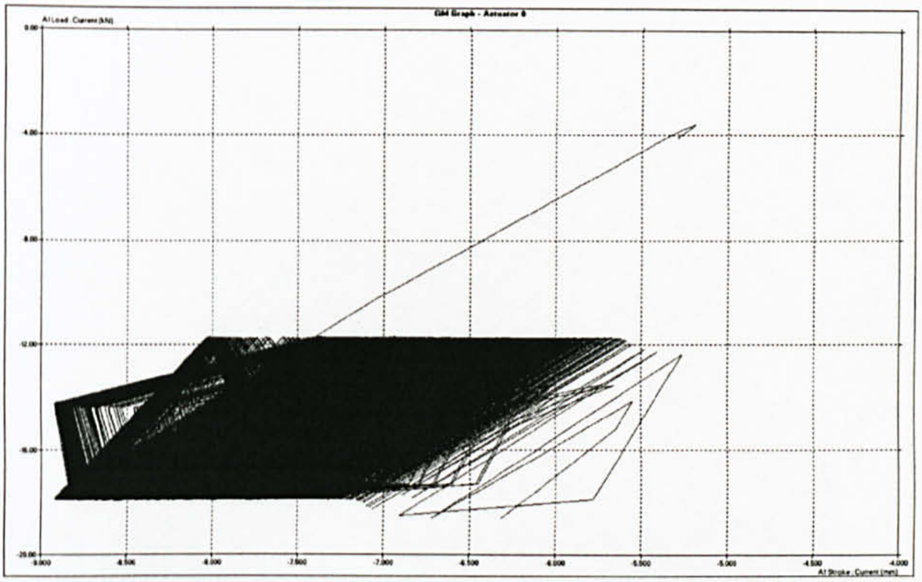

   b) Cycles done = 144000

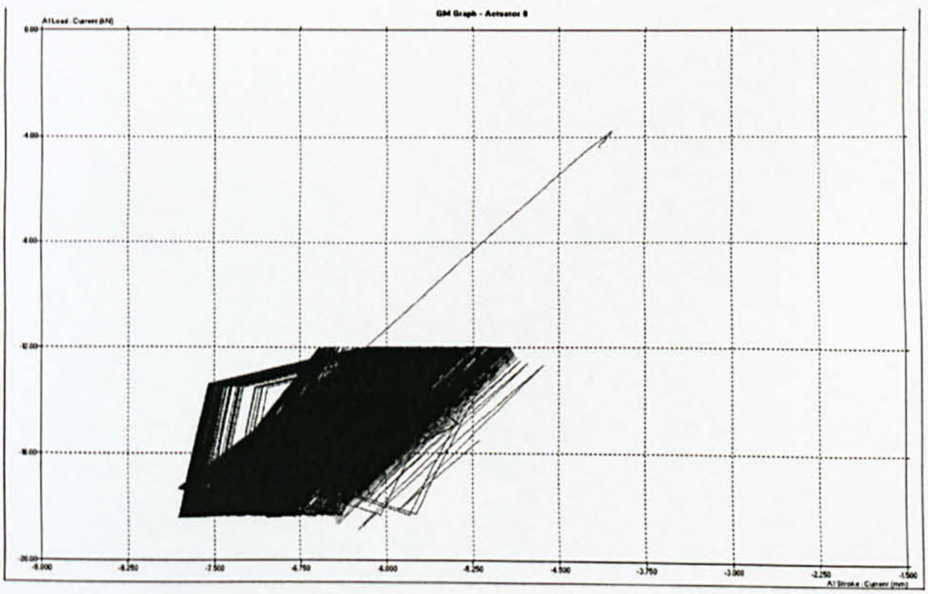

Total cycles done for GFST Beam (1.20Pult/0.2Pult): Cyclic load graph for 1.2m length, 3.2mm thickness = **288000**

APPENDIX C: FIGURES

1) BARE BEAMS AND GFST BEAMS SUBJECTED TO STATIC LOAD TESTING

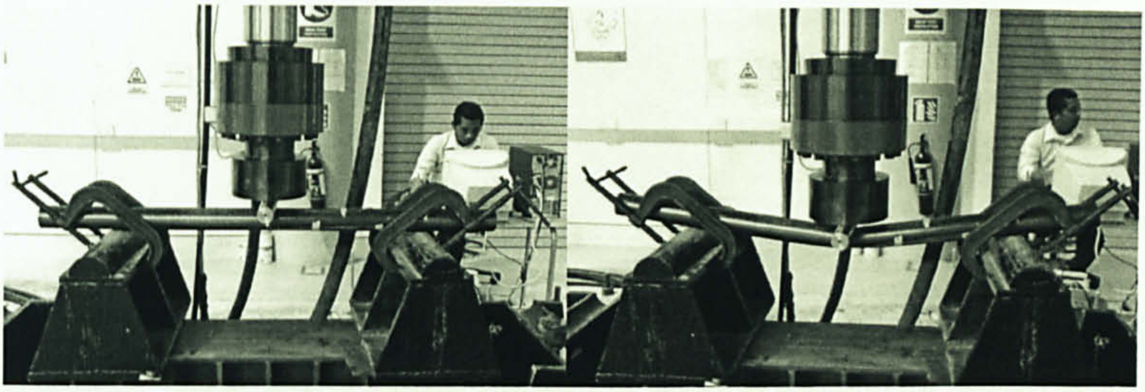

Figure C- 1: Behavior of the beam before and after static load test

Figure C- 2: Comparison of failure mode between bare beams and GFST beams with different value of thickness

2) BARE BEAMS AND GFST BEAMS SUBJECTED TO CYCLIC LOAD TESTING

Figure C- 3: Effect of cyclic load on bare beam and GFST beams